Atmosphere

Atmosphere

Contents

Canadian Meteorological Societ
Société Météorologique du Canad

On Truncation Errors in Sigma-System Models[1]

Hilding Sundqvist
Dynamic Prediction Research Division
Atmospheric Environment Service[2]
Montreal, Quebec

ABSTRACT

A detailed examination is given as to how temperature T – and thus geopotential – of a synoptic state appears in sigma(σ)-coordinate systems, i.e., systems whose lowest coordinate surface coincides with the earth's surface. It is shown that the description of T along constant σ requires many more Fourier modes than would be expected by merely regarding the horizontal synoptic variation. This effect is related to the scale of the orographic field and to the vertical variation of T. With these results as a basis, possible truncation errors – directly associated with the use of σ-coordinates – of horizontally discretized functions are discussed. It is found that if the resolution is inadequate, horizontal advection in the thermodynamic equation may become significantly distorted as a result of truncation. It is furthermore inferred that, with proper difference formulation of the terms of the pressure gradient force, it ought to be possible to limit – though not to eliminate – errors in this quantity.

To illustrate the theoretical/qualitative deductions, a few numerical applications are carried out. These also indicate that the maximum truncation error in the pressure force would be about $0.5\ \mathrm{ms}^{-1}$, expressed as equivalent geostrophic wind at mid-latitudes. This figure was obtained with centered difference (second order accuracy) approximation of derivatives, a grid distance of 370 km and a ground slope corresponding to that on the western side of the Rocky Mountains.

1 Introduction

In conjunction with the use of coordinate systems whose "horizontal" surfaces follow the terrain – such as the sigma system, first proposed by Phillips (1957) and variants of this (Smagorinsky, 1965; Arakawa, 1972) and the normalized height coordinate system (Kasahara, 1974) – it is occasionally noted that functions, when horizontally discretized in these systems, may suffer from appreciable horizontal truncation errors. These appear primarily in regions where the earth's orography has sharp gradients, which consequently yield equally sharp gradients in pressure, temperature and geopotential along the horizontal coordinate sur-

---

[1]Contribution number 310.
[2]Present address: Dept. of Met., Arrheniuslab., Fack, S-104 05 Stockholm 50, Sweden.

faces. (Henceforth, chiefly the sigma system will be referred to, as it may represent the terrain following coordinate systems; furthermore, when there is no risk of ambiguity, "horizontal" will be used for either of: along constant altitude, constant pressure or constant sigma.)

Smagorinsky et al. (1967) reported on problems with truncation errors of the above-mentioned kind when orography was introduced into the general circulation model of the Geophysical Fluid Dynamics Laboratory, Princeton. They also suggested that the pressure gradient force be calculated in the p-system in order to suppress the errors. This technique appears to serve the purpose, as shown by comparative experiments (Kurihara, 1968). Gary (1973) studied the truncation errors by numerical evaluation of these in both the z-system and the σ-system. However, his paper does not fully clarify the reasons why truncation errors are likely to be larger in the σ-system than in the z- or p-systems. Corby et. al. (1972) present an analysis of how to design the finite difference formulation of the pressure force to efficiently suppress errors in the case of temperature varying linearly with log of pressure. Phillips (1974) also discusses the truncation error of the pressure gradient force in a recent paper, upon which we shall comment further later on.

Now, as a result of discretization, truncation errors always arise, because the functions are truncated beyond a certain wave number and because the components of the highest possible wave numbers of a particular resolution are poorly described. Hence, if we consider the truncation error to be undesirably large, the implication is that the amplitudes of the highest wave numbers of the function(s) involved are of significant magnitude. This phenomenon appears to be particularly pronounced in the σ-systems. None of the above-mentioned papers elaborates on this matter. For the purpose of gaining some further insight as to how horizontal truncation errors arise in σ-systems, we shall investigate the origin of the high wave-number components and their effects on various evaluations.

The p- and z-systems have a meteorologically natural separation of the coordinate axes in that a variable's horizontal fluctuations essentially are related to the synoptic state and in that the basic hydrostatic variation may be described with a good degree of accuracy as a variation along the vertical axis only. Therefore, the p-system is used as a reference in the present investigation. We shall consider a simple, well defined atmospheric state in the p-system, and then in some detail look into the consequences of a transformation to the σ-system, taking the existence of orography into account.

The transformation from p to σ yields rather complex relations, despite starting from a simple structure. The formal analytical expressions that could be derived do not permit us to draw clear conclusions. Consequently, the present study includes qualitative discussions and numerical examples.

2 Qualitative Effects of p- to σ-transformations

a *Temperature*

Let us begin this discussion by considering the pressure gradient force, which

takes the form

$$FP = \nabla_p \phi \qquad (1)$$

in the p-system, and

$$FS = \underset{\text{I}}{\nabla_\sigma \phi} + \underset{\text{II}}{RT\nabla \ln p_s} \qquad (2)$$

in the σ-system. The variables in (1) and (2) have their conventional meaning, and the subscripts p and σ indicate that the evaluation is performed keeping p and σ, respectively, constant. In regions with pronounced orographic gradients, the two terms I and II of (2) may individually be 10–20 times larger in magnitude than a typical value of their sum – which in the analytic case is identical to (1). Hence, if for some reason, the temperature in (2) deviates by 1% ($\sim$2–3°C) from the correct value, a 10–20% error in the pressure gradient force will arise. In the light of this general sensitivity to the determination of temperature, we shall proceed to looking at its description in the σ-system.

In view of what was said in the introduction (third paragraph) and in view of the fact that in practice we get the initial fields from analyses performed in the p-system, we shall start from a temperature distribution given in the p-system. Thus, let us consider

$$T = T_0 + \sum_{n=1}^{N} \gamma_n z^n \qquad (3)$$

where

$$z = \ln \frac{p}{p_0}; \quad (p_0 = 1000 \text{ mb})$$

For the moment, we assume that T_0 and γ_n are independent of the horizontal coordinates. In order to fairly realistically describe T – i.e., to include tropopause and other inversions – by (3), we generally need to take $N = 3$ or 4. Let us furthermore assume that we have an orographic structure such that the horizontal variation of $\ln p_s$ may be represented by one Fourier component (for simplicity we shall henceforth take only x-variations into account):

$$\ln \frac{p_s}{p_0} = z_s = -\hat{P}_m \left(1 - \cos \frac{2\pi m}{D} x \right) \qquad (4)$$

where m is the wave number and D is the size of the domain. Using the definition of $\sigma (= p/p_s)$ we may write

$$z = \ln \sigma + z_s \qquad (5)$$

Inserting (5) in (3) we obtain an alternative T-description that is applicable to the σ-system:

$$T = T_0 + \sum_{n=1}^{N} \gamma_n (\ln \sigma + z_s)^n$$

$$= T_0 + \sum_{n=1}^{N} \gamma_n \left(\ln \sigma - \hat{P}_m + \hat{P}_m \cos \frac{2\pi m}{D} x \right)^n. \qquad (6)$$

From expansion (6) we find that, along constant σ, T has an x-variation whose description requires not only the basic orographic wave number m but all wave numbers up to Nm. With the specific assumptions made here, it is of course only those modes of exact multiples of m that appear, while in a more complex (realistic) case, where a summation over m is needed, a more diffuse distribution along the wave number axis will result. In this pure example it is clear that the spectral distribution of T in the σ-system is a consequence of the fact that the vertical temperature variation partially appears as a variation along σ-surfaces because these are tilted with respect to p-surfaces.

Including a synoptic-scale variation in T_0 and γ_n

$$T_0 = \sum_{l=0}^{L} \hat{T}_{0l} \exp \left(i \frac{2\pi l}{D} x \right) \tag{7a}$$

$$\gamma_n = \sum_{l=0}^{L} \hat{\gamma}_{nl} \exp \left(i \frac{2\pi l}{D} x \right) \tag{7b}$$

we notice that T_0 (7a) will simply be superimposed, while γ_n may yield amplitudes of still higher wave numbers $(Nm + l)$. Accordingly, having the same grid point separation (Δs) in the σ-system as in the p-system, we have reasons to expect a more severe truncation error of temperature in the former than in the latter.

In view of the preceding analysis, we find it pertinent to regard two aspects of the truncation problem of temperature. Firstly, smaller scale (yet reasonably well represented by the horizontal expansion) synoptic features, may be truncated or misrepresented by aliasing as a result of the coordinate transformation from p to σ. Secondly, once the transformation is performed, there may exist amplitudes of significant magnitude in the highest representable wave numbers (corresponding to wavelengths two to four Δs). This second aspect will affect the accuracy of a subsequent time integration of the thermodynamic equation, because of possible aliasing in the non-linear horizontal advection terms, and because the advection of short-wave components is poorly approximated. How severe these effects are, may possibly depend on whether temperature or potential temperature is used as prognostic variable. A more detailed investigation of this particular matter requires that the full dynamical system be considered, so we shall here be content with the qualitative inferences just made.

b *Pressure gradient force*

Turning to a closer examination of the pressure gradient force (2) and its evaluation, we shall first realize that term I as well as term II in (2) is a function of temperature. This implies that both terms I and II contain the high wave number components of T and that these – ideally – cancel, leaving FS with merely the synoptic scale. Consequently, we ought to experience the same net truncation error of this term in the σ-system as in the p-system. Why does this not seem to be the case?

To give an answer to this question, it is illustrative first to regard the situation

in an isothermal atmosphere. Then, we readily realize, the components of II in (2), which result from orography, will have an exactly (except for possible round-off errors) cancelling counterpart in term I. This is true, whatever the spectral distribution of the orographic field might be, because the two terms are subject to exactly the same truncation in this case.

Then, taking a more general situation, by considering a temperature distribution according to (6), the associated geopotential field is

$$\phi = \phi_0 - RT_0(\ln \sigma + z_s) - R \sum_{n=1}^{N} \frac{\gamma_n}{n+1} (\ln \sigma + z_s)^{n+1} \tag{8}$$

If we again for simplicity assume ϕ_0, T_0 and γ_n to be independent of x (i.e., $FP \equiv 0$); the second order difference approximation to the derivative of ϕ (term I of FS) implies the following expression

$$\phi_x = - \frac{R}{2\Delta s} \left\{ T_0(z_{sj+1} - z_{sj-1}) \right.$$
$$\left. + \sum_{n=1}^{N} \frac{\gamma_n}{n+1} \left[(\ln \sigma + z_s)_{j+1}^{n+1} - (\ln \sigma + z_s)_{j-1}^{n+1} \right] \right\} \tag{9}$$

where $j = x/\Delta s$.

A tentative expression for term II of FS would be

$$RT(\ln p_s)_x = \frac{R}{2\Delta s} \left[T_0 + \sum_{n=1}^{N} \gamma_n (\ln \sigma + z_s)^n \right] (z_{sj+1} - z_{sj-1}) \tag{10}$$

Adding (9) and (10) with $\gamma_n = 0$ yields a verification of the statement in the preceding paragraph. If, on the other hand, $\gamma_n \neq 0$ we note that it is quite likely that the non-linear terms in (9) and (10) will be differently truncated. Thus, we may answer the question posed above by stating that an additional truncation error of the pressure gradient force – as compared to the p-system – arises in the σ-system as a result of inconsistent truncation of the individual terms I and II in (2). This was also pointed out by Smagorinsky et al. (1967). This specific problem is circumvented by their proposed method mentioned above (Section 1). Their method may have disadvantages, however – in addition to the practical ones – in that geopotential has to be extrapolated in certain regions at the top and the bottom of the model atmosphere.

The preceding analysis, may give some guidance as to how FS should be evaluated in order to minimize the truncation error. It is not the intention of the present study to dwell upon numerical formulations, but we shall merely make a couple of observations. For $N = 1$, that is for T varying linearly with $\ln p$, we find that (10) becomes identical to (9) (with opposite sign) if the mean value of T from $(j + 1)$ and $(j - 1)$ is applied in (10). This conclusion was also reached by Corby et al. (1972). For $N > 1$, we can no longer expect to find a formulation of (10) that exactly matches that of (9). However, the $N = 1$ case indicates, that with a suitable form of (10), the error could still be kept within tolerable limits. Furthermore, it appears that the accuracy can hardly be increased by subtracting some kind of a basic state, such as an isothermal one or one with a linear $\ln p$

variation of T, from the terms in (2) because it is the higher vertical modes that cause the difficulties in the difference formulations.

Note that an analytic form of $T(p)$ has been used in the preceding discussion. The possible influence of vertical truncation in relating T and ϕ is thus excluded. The vertical truncation will be discussed briefly in the following paragraphs.

c *On representation and truncation in the vertical*

It might, as a first obvious thought, appear that the problems discussed above would have been more or less eliminated if temperature had been expanded, instead of (6), as

$$T = T_s + \sum_{n=1}^{N} \gamma_n'(\ln \sigma)^n \tag{11}$$

where T_s is the temperature at the surface, *i.e.* at $\ln \sigma = 0$, $z = z_s$. However, this is not the case. We shall not do a detailed examination of this, but it seems sufficient to merely regard the geopotential as it is obtained by integrating the hydrostatic equation using (11) and (5): *i.e.*

$$\phi = \phi_s + RT_s(z - z_s) + R \sum_{n=1}^{N} \frac{\gamma_n'}{n+1} (z - z_s)^{n+1}. \tag{12}$$

From (12) and some additional algebra we realize that, for a given $\phi_s \neq 0$ to which T_s and z_s are related, $(\partial\phi/\partial x)_p$ cannot become equal to zero for $\gamma_n' \neq 0$ unless these are composed of several wave numbers in an expansion along the x-axis. The generality of the foregoing discussions is consequently not restricted because we chose the p-system as a reference from which we derived the σ-system expressions.

So far, we have been regarding analytical forms for the vertical variation of the dependent variables. Quite naturally, the question arises as to how a discretization in the vertical affects the truncation errors considered above.

Since the vertical variation of the variables partly appears as high frequency variations along the σ-surfaces, we can infer that, for a given horizontal resolution, the horizontal truncation error increases as the vertical resolution increases. The vertical discretization does not, in principle, cause any enhancement of the horizontal truncation error, once the transformation to the σ-system is completed. However, there is an important aspect of this problem in conjunction with the transformation (interpolation) from p to σ, when one has to resort to a finite number of levels. A separate report on this question is under preparation, so we shall only briefly bring up a few points here, which are pertinent in the present context.

Let us for simplicity assume that we have an analytic expression for the hydrostatic relation between T and ϕ, which we use only to specify ϕ of the desired σ-levels. Then, in the discrete σ-representation, a finite difference form of the hydrostatic relation gives $T(\sigma)$. Generally this $T(\sigma)$ will, as a result of vertical truncation, deviate from the T we would find by using the analytic expression. (T and ϕ could of course be interchanged in the foregoing reasoning.) Con-

sequently, regarding the calculation of the pressure gradient force (2), an error will appear as a horizontal truncation error, while in fact it originates from vertical truncation yielding inconsistencies between T and ϕ in conjunction with transfer of data from p to σ coordinates. This error would appear even if we had analytic expressions for the variables in the horizontal. On the other hand, once the interpolation is completed, this error will not be re-introduced during a following time integration. This means that if we can design the interpolation procedure such that the consistency between T and ϕ is preserved, no further attention to this specific error is needed.

This consistency problem is the basic question of Phillips' study (1974). In this, Phillips also demonstrates by a few alternative numerical examples how substantial errors may arise in the horizontal pressure force term and he considers those errors being due to horizontal truncation in the σ-system. However, Phillips considers a discrete representation in the vertical. Therefore in view of the present discussion, it is quite likely that the errors he obtains are partly due to vertical truncation as discussed in the preceding paragraph and partly due to the 'pure' horizontal truncation investigated in Section 2b.

3 Numerical Examples

In order to obtain a general, quantitative measure of the effects discussed in section 2, we shall look at a few simple numerical examples.

For this purpose we consider an atmosphere in which $FP \equiv 0$ (eqn. 1) and in which T varies piece-wise linearly with $\ln p$. The hydrostatic equation can thus be integrated analytically to find ϕ at any pressure (or sigma) level. This implies that no errors of the kind discussed in 2c will appear. Instead of specifying $\ln p_s$ as was done for simplicity in Section 2, eqn. (4), we now specify the geopotential of the earth's surface as

$$\phi_s = \tfrac{1}{2}\hat{\phi}_m\left(1 - \cos\frac{2\pi m}{D}\,j\Delta s\right) \; ; \quad j = 0, 1, ..., J. \tag{13}$$

Unless specially remarked, we let ϕ_s vary according to (13) across the whole domain, D. From (13) and the hydrostatic relation we then retrieve $\ln p_s$ ($= z_s + \ln p_0$) from

$$\frac{R\gamma_0}{2}\,z_s{}^2 + RT_0 z_s = -(\phi_s - \phi_0) \tag{14}$$

where γ_0 is a fixed lapse rate for pressures greater than p_s. We shall assume $\phi_0 = 0$ in most of the examples.

After having calculated $\ln p_s$ and T, $T_x(= \partial T/\partial x)$, ϕ and FS along a given σ-level and for a given vertical profile of temperature, we then Fourier analyze these functions. All amplitudes are then related to the maximum amplitude of the expansion; the mean value of the function (amplitude of wave number zero) is excluded however. These normalized amplitudes will for convenience be denoted by a carat and a subscript k for wave number (e.g., $(\widehat{\ln p}_s)_4$); no distinction is made between sine and cosine amplitudes. Actual grid point values

of the pressure force will naturally be examined as well. Derivatives are approximated by centered differences (second order accuracy), except for $j = 0$ and $j = J$ where one-sided differences are taken. The handling of the temperature multiplying $\partial \ln p_s/\partial x$ will be described later on.

In the experiments to be presented, the parameters have the following values:

$T_0 = 288 \, °K$;

γ_0 approximately corresponding to the standard atmosphere lapse rate;

$D = 10^7 \, m$;

$\phi_m = 2100 \cdot 9.8 \, m^2 s^{-2}$;

$m = 4$.

Furthermore, $J = 75$ is considered as a reference resolution; this implies $\Delta s = 133$ km and an orographic wavelength, $L_m = 18.8 \, \Delta s$.

As the relation (14) between z_s and ϕ_s is non-linear, the Fourier expansion of z_s contains coefficients in the wave numbers k that are multiples of m, although the coefficients are very small for $k > m$. Hence in percent, $\hat{z}_{s4} = 100, \hat{z}_{s8} = 0.67$, $\hat{z}_{s12} = 0.01$ and for $k \neq 4, 8$ and $12 \, \hat{z}_{sk} \sim 10^{-3}$ and smaller.

In the first couple of experiments, lapse rate γ, is set constant throughout the depth, i.e., $\gamma \equiv \gamma_0$. Consequently, it is irrelevant which σ-level is chosen for an examination of the associated functions.

In agreement with the discussion in section 2.1 ($N = 1$ in (6)), T has a spectral distribution similar to that of $\ln p_s$; $\hat{T}_4 = 100$, $\hat{T}_8 = 0.67$ and for all other k, $\hat{T}_k < 10^{-2}$. The same typical feature also shows up in T_x. However, $T_x \neq 0$ (because $\gamma \neq 0$), and therefore, truncation caused by the difference approximation excites not only those components that are multiples of m, but all others as well. The results are: $(\hat{T}_x)_4 = 100$, $(\hat{T}_x)_8 = 1.27$ and $(\hat{T}_x)_k \simeq 0.46$ for all other k.

Regarding the pressure gradient force FS and referring to the discussion in section 2.2, the temperature multiplying $(\ln p_s)_x$ is averaged as

$$\bar{T}_j = \tfrac{1}{2}(T_{j+1} + T_{j-1}) \tag{15}$$

The resulting FS – measured in equivalent geostrophic wind at lat. $45°$ – has a magnitude that is no greater than $10^{-11} \, ms^{-1}$. In another run, instead of (15), $\bar{T}_j$ was defined as

$$\bar{T}_j = \tfrac{1}{3}(T_{j+1} + T_j + T_{j-1}) \tag{16}$$

Then the maximum error in FS was found to be about $6 \times 10^{-2} \, ms^{-1}$. This may still be regarded a very small error, but nevertheless, it does exhibit the importance of how temperature is treated in the term in question.

This set of experiments was repeated, but with $J = 27$, i.e., $\Delta s = 370$ km and $L_m = 6.8\Delta s$; these values are fairly representative for models in NWP. The temperature distribution is practically the same as in the preceeding resolution. For T_x, on the other hand, the coarser resolution is reflected in that there are now no $\hat{T}_x$ smaller than ~ 3.8. This is an increase that should be expected with the second order accuracy approximation.

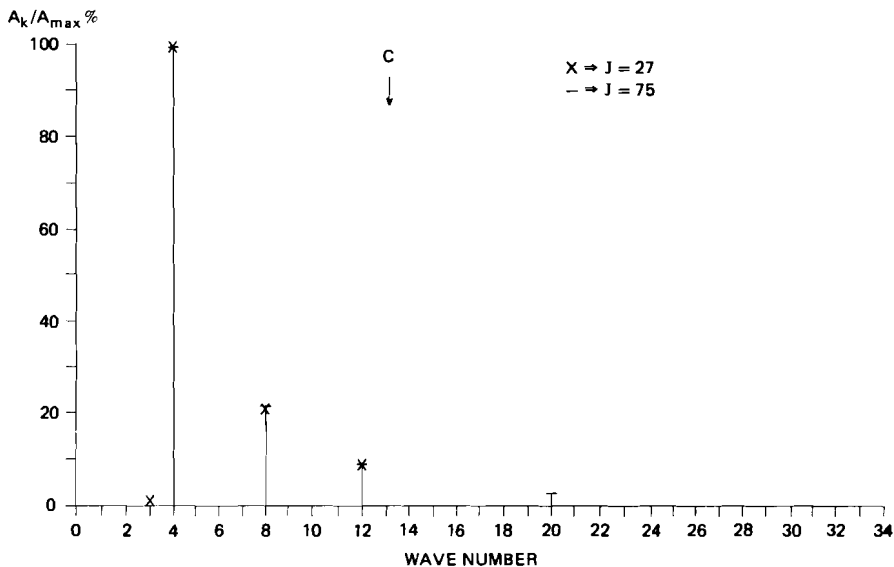Using expression (15) for $\bar{T}_j$ in FS, again yields errors no greater than 10^{-11}

Fig. 1 Normalized spectrum of temperature (wave number zero excluded). Notations: crosses denote the coarser resolution ($J = 27$) and bars the finer ($J = 75$). Mark C shows the highest wave number for $J = 27$. (The wave numbers for $J = 75$ are shown only to 34 instead of 37).

ms^{-1}. If, on the other hand, $\overline{T}_j$ according to (16) is employed, a maximum error of about 0.4 ms^{-1} arises. We shall comment on this together with other results below.

In the next block of calculations, a temperature inversion and a tropopause were introduced as follows

$$\begin{aligned} \gamma &= \gamma_0 \text{ for } 1000 \geqslant p \geqslant 750 \text{ and } 650 \geqslant p \geqslant 250 \text{ mb} \\ \gamma &= 0 \ \ \text{ for } \ \ 750 \geqslant p \geqslant 650 \text{ and} \qquad p \leqslant 250 \text{ mb} \end{aligned} \tag{17}$$

This stratification corresponds to $N > 1$ in the symbolical vertical variation (6), upon which we based the qualitative discussions in section 2.

The functions were computed on σ-levels 0.1, 0.3, ..., 0.9. Since p_s ranges between 1000 and 775 mb, we find that $\sigma = 0.1$ and $\sigma = 0.5$ are both situated in layers where γ has one value only. Consequently, the results at those levels are similar to the results just presented. The evaluations on the other σ-levels produce results, the typical features of which are common for all those levels. The specific values shown here are taken from $\sigma = 0.7$.

The distribution of $\widehat{T}_k$ is shown in Fig. 1 for both $J = 75$ and $J = 27$. The existence of components of wave numbers that are multiples of m appears clearly. We furthermore notice that temperature is well represented also in the coarser resolution as far as the spectrum reaches.

Regarding T_x, we find that a noticeable truncation occurs for the case $J = 27$, as revealed by Fig. 2. What is even more important to observe concerning this
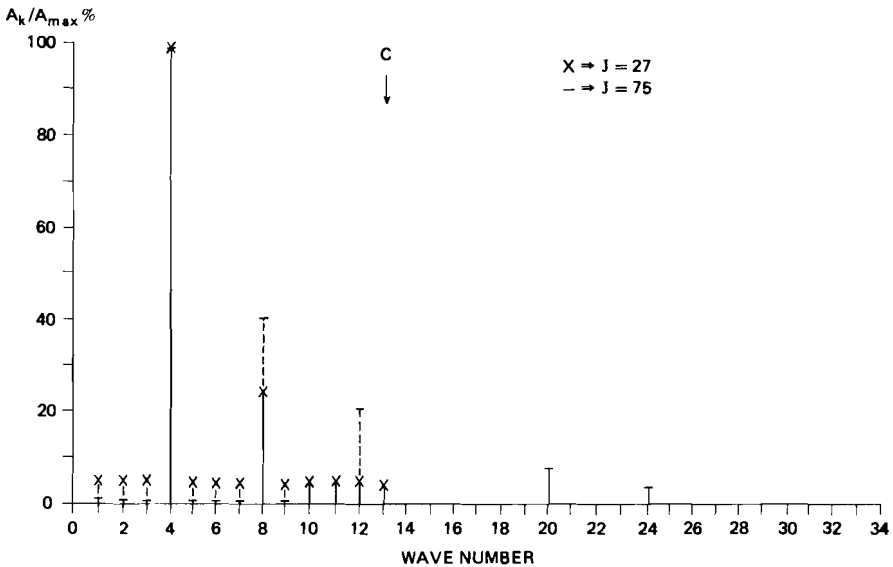
On Truncation Errors in Sigma-System Models   89

Fig. 2 Normalized spectrum of $\partial T/\partial x$ along σ-constant (wave number zero is excluded). Notations as in Fig. 1.

resolution is that a significant contribution ($\sim 25\%$ of the largest component) to T_x comes from the relatively high wave number, $k = 8$. This corresponds to a wave length of $3.4\Delta s$. Consequently, temperature changes brought about by horizontal advection would be, to a significant degree, poorly described. To further accentuate the importance of this, we may realize that, in a 10 ms^{-1} flow across a mountain range with a slope like that of the Rocky Mountains, the advection along σ-constant has a magnitude corresponding to a temperature change of the order 10°C/day. Of course, in general there are other and compensating terms in the thermodynamic equation and the net change is much smaller. However, all those terms are likely to be inconsistently truncated so the errors may still become noticeable.

In the calculation of FS both the expressions (15) and (16) for temperature averaging were tested. In section 2.2, we deduced that with T varying non-linearly with $\ln p$, (as the case is here around $\sigma = 0.7$) the form (15) no longer is as perfect as it is in the case of linear variation. This is indeed confirmed by the calculations. Using (15) the maximum error (measured as before) in FS is 0.45 ms^{-1} for $J = 75$ and 0.98 ms^{-1} for $J = 27$, whereas the error is reduced to 0.18 ms^{-1} and 0.52 ms^{-1} when (16) is employed. These latter values are just slightly larger than those obtained with (16) in the preceding evaluations (T linear in $\ln p$).

In order to get a quantitative picture for the case of a more realistic orography field, ϕ_s was then given by only one full wave length according to (13) and placed around the mid point of the domain D and in the rest of D, $\phi_s \equiv 0$. Other param-

eters were the same as in the last presented experiments, *viz.*, γ according to (17) and in FS (16) was used. The ϕ_s field so defined does, of course, no longer consist of merely one Fourier component. Therefore a smoothing was applied to suppress the highest modes in each resolution. The spectral distribution – presented in the same way as for the other functions – of ϕ_s is depicted in Fig. 3.

The same typical features as in the previous cases concerning spectral distribution and truncation of T and T_x appear here too, although the spreading is more diffuse because ϕ_s contains several wave modes. This is shown in Figs. 4 and 5 respectively.

The maximum error in FS is 0.18 ms^{-1} for $J = 75$ and 0.40 ms^{-1} for $J = 27$. The latter error is smaller than the corresponding one in the preceding experiments. This is apparently due to the smoothing applied to ϕ_s here.

The spectral distribution of FS for this case is displayed in Fig. 6. We notice that the same characteristic periodicity, as that of T and T_x, along the wave number axis stands out here as well. Although the modes of FS that correspond to those of ϕ_s (Fig. 3) are the most pronounced ones, we observe that relatively large contributions also come from other (higher) modes. The error in FS significantly excites scales all over the spectrum of a given resolution.

Other numerical experiments have been performed, where for example synoptic-scale variations were imposed on T_0, ϕ_0 (eqn. 14) and the stratification. However, such variations add very little to the magnitude of T and ϕ variations along σ-surfaces in the presence of orography. Therefore, nearly similar characteristics, as presented already, emerge. Nevertheless, it seems worth mentioning that the magnitude of the FS-error remains practically the same as in the cases just presented.

The examinations of the kind carried out here, where attention chiefly is paid to series expansions, give the impression that observed features are global. This is somewhat misleading in the present case. The short wave components of T_x and the errors in FS essentially appear (or at least originate) in layers containing vertical variation of the lapse rate (e.g., the tropopause) in the vicinity of pronounced orographic gradients.

4 Summary

Let us finally summarize the most essential conclusions and results of the present study of some possible truncation errors and their origin in models with sigma as vertical coordinate, as follows.

Part of the variation of temperature and/or geopotential along the vertical appears as a horizontal (along $\sigma = $ constant) variation in σ-systems. Therefore, we find that a higher horizontal resolution is required in the σ-system than in the *p*-system to describe the instantaneous horizontal derivatives of the internal atmospheric state with the same detail in the two systems. This fact has an impact on the accuracy with which the horizontal temperature advection and the pressure force in the σ-system can be evaluated in discretized form.

Truncation errors that are due to the use of σ-coordinates may be completely avoided in the pressure gradient force term, irrespective of resolution, if the lapse
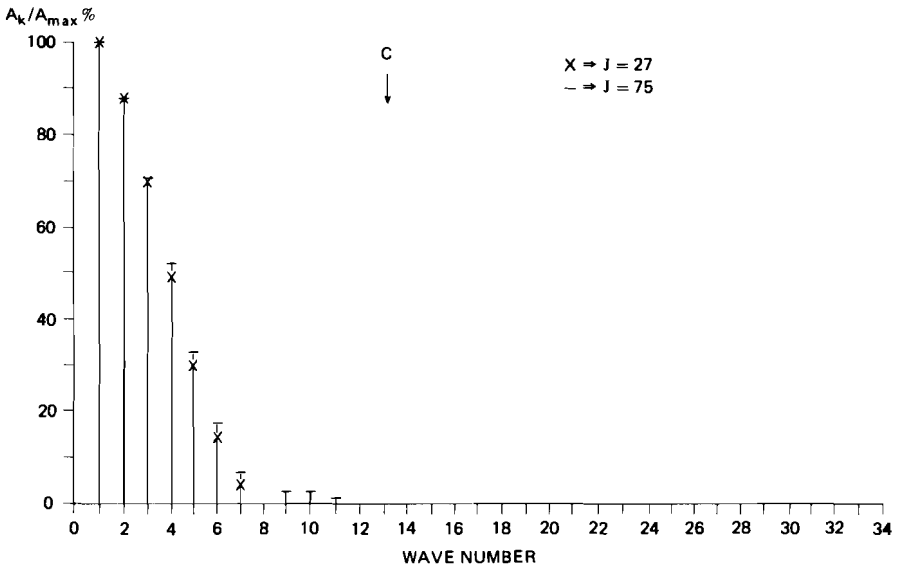
Fig. 3   Normalized spectrum of ϕ_s for "realistic" orography described in text (wave number zero excluded). Notations as in Fig. 1.
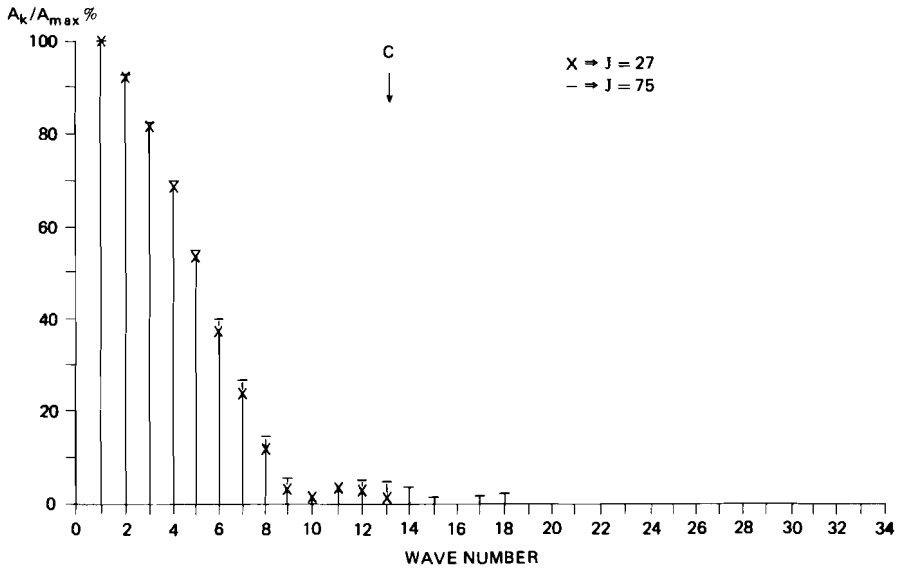

Fig. 4   Normalized spectrum of temperature for the ϕ_s-case shown in Fig. 3 (wave number zero excluded) Notations as in Fig. 1.
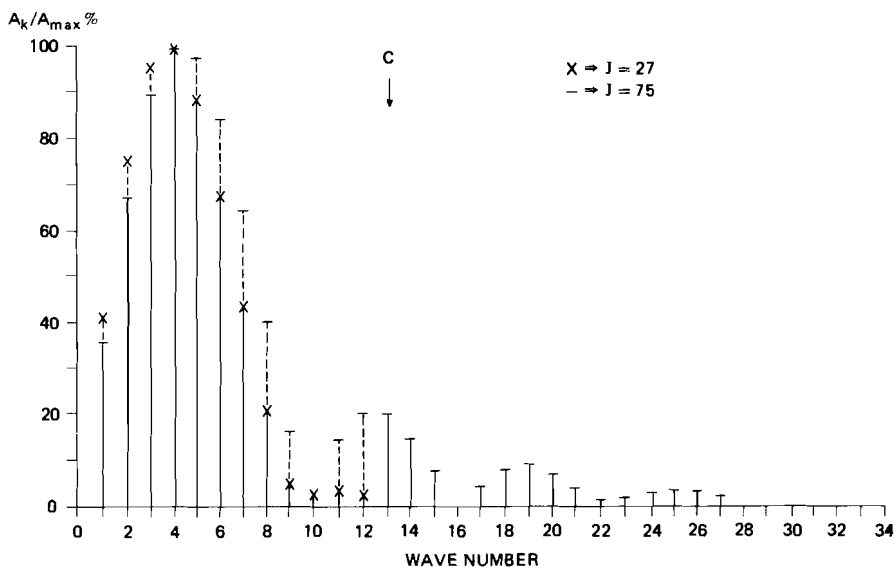
Hilding Sundqvist

Fig. 5 Normalized spectrum of $\partial T/\partial x$ along σ-constant in the ϕ_S-case shown in Fig. 3 (wave number zero excluded). Notations as in Fig. 1.
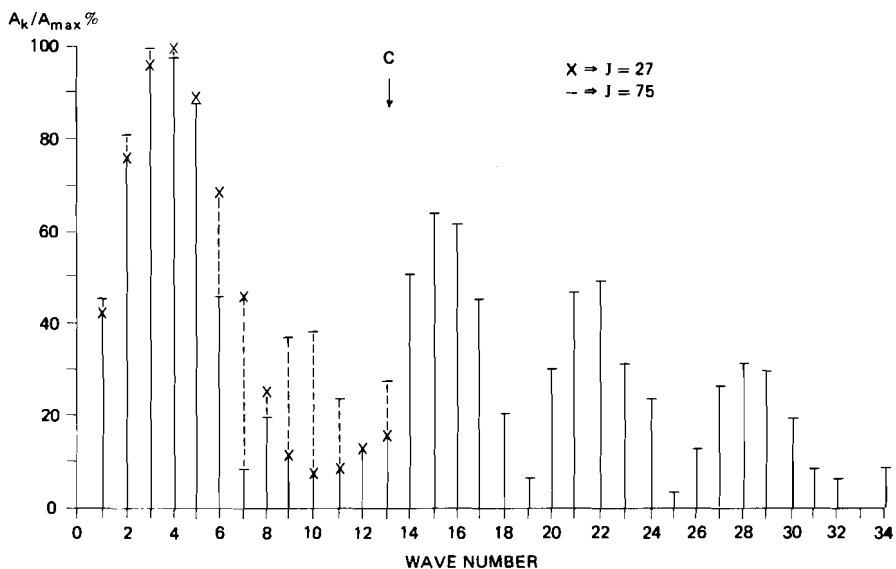

Fig. 6 Normalized spectrum of FS in the ϕ_S-case shown in Fig. 3 (wave number zero excluded). Notations as in Fig. 1.

On Truncation Errors in Sigma-System Models   93

rate is constant through the whole depth of the atmosphere. In a more realistic case with a tropopause and other inversions present, it appears that a certain truncation error is inescapable. However, the present numerical experiments indicate that, with a careful difference formulation, this error can be kept within tolerable limits. An optimum formulation will depend on the design of the difference scheme of a model. With $\Delta s \sim 300$–400 km, the error would be equivalent to about 0.5 ms^{-1} geostrophic wind where the ground slope corresponds to that of the Rocky Mountains in numerical models. This magnitude of the error is generally smaller than what Phillips (1974) obtained. This discrepancy is probably due to the fact that vertical truncation also contributed to the error magnitude in Phillips' calculations. The quantitative examples furthermore indicate that this error decreases more slowly with increasing resolution than usually may be expected in a given difference approximation.

As a rough guidance regarding the relation between model resolution and orographic scales it seems advisable not to allow amplitudes of significant magnitude for wave-lengths shorter than 8–$10\Delta s$ in the orography field. (This would correspond to $J = 32$–40 in the preceding experiments.) Such a resolution results in a much more moderate truncation for wave numbers less than 12, than does the $J = 27$ case in the present experiments. Supplementary experiments with a complete dynamical model system would enable a more precise recommendation in this respect.

The specific effects on the meteorological variables in σ-systems originates in the vicinity of marked orographic slopes and are specially pronounced in atmospheric layers containing inversions.

Truncation errors caused by discrete description in the vertical have not been examined here. But a brief discussion (Section 2c) shows that such errors may be investigated separately and that the results of the present study do not suffer in generality because of such a separation.

In this investigation of truncation effects, we have merely regarded temperature and geopotential. Effects of the kind studied here will, in principle, appear in the wind and moisture fields as well. These effects would probably show up most clearly in the moisture because it often has abrupt changes in the vertical variation, like temperature has.

In comparison to the p-system, sigma systems are advantageous because the earth's surface is always a coordinate surface in these systems. It furthermore seems appropriate to remark that problems analogous to those exhibited and discussed in the present study also appear in p-system models with orography included (see e.g., Katayama *et al.* 1974).

Although the present study concerns horizontally discretized functions we shall close with an observation applicable to spectral models. The major motivation for the use of such models lies in their computationally accurate calculation of horizontal derivatives within the spectrum covered by the resolution. In view of the present analysis, that advantage over grid point models appears to be even more outstanding regarding the thermodynamic (and moisture) equation in models using σ as vertical coordinate. Furthermore, with reference to the

difference expressions (9) and (10) the pressure force will be given correctly in spectral models because there is in this case a perfect matching of the cancelling parts that come from each of the two terms of the pressure force.

Acknowledgements

References

ARAKAWA, A., 1972. Design of the UCLA general circulation model. Tech. Rpt. No. 7, Dept. of Meteor. UCLA.

CORBY, G.A., A. GILCHRIST, and R.L. NEWSON, 1972. A general circulation model of the atmosphere suitable for long period integrations. *Quart. J. Royal Meteor. Soc.*, **98**, 809–832.

KATAYAMA, A., Y. KIKUCHI, and Y. TAKIGAWA, 1974. MRI Global 3-level model. GARP Publications Series, No. 14, 174–188.

GARY, J., 1973. Estimate of truncation error in transformed-coordinate primitive-equation atmospheric models. *J. Atm. Sci.*, **30**, 223–233.

KASAHARA, A., 1974. Various vertical coordinate systems used for numerical weather prediction. *Mon. Weather Rev.*, **102**, 509–522.

KURIHARA, Y., 1968. Note on finite difference expressions for the hydrostatic relation and pressure gradient force. *Mon.*

Weather Rev., **96**, 654–656.

PHILLIPS, N.A., 1957. A coordinate system having some special advantages for numerical forecasting. *J. Met.*, **14**, 184–185

——, 1974. Application of Arakawa's energy-conserving-layer model to operational numerical weather prediction. US Dept. of Commerce, NMC, Office Note 104.

SMAGORINSKY, J., S. MANABE, and J.L. HOLLOWAY, 1965. Numerical results from a nine-level general circulation model of the atmosphere. *Mon. Weather Rev.*, **93**, 727–768.

SMAGORINSKY, J., and Staff Members, 1967. Prediction experiments with a general circulation model. Proceedings of the International Symposium on Dynamics of Large-Scale Processes in the Atmosphere (IAMAP/WMO), Moscow, USSR, 1965.

Climatic Teleconnections with the Equatorial Pacific and the Role of Ocean/Atmosphere Coupling[1]

Hermann Flohn and Heribert Fleer
Meteorologisches Institut der Universität Bonn

[Manuscript received 7 August 1975]

ABSTRACT

Starting from the occurrence of a zonal Walker circulation supplementing the meridional Hadley cell, the concept of ultralong waves with diagonal upper troughs extending far into the Tropics is stressed. The model of equatorial upwelling with air-sea coupling is critically discussed and a modification proposed. An intensification of the subtropical jet at the peak of the 1972 El Niño (as suggested by Rowntree's model calculations) has been verified.

Empirical studies deal with the large interannual and interdecadal variations of the energy fluxes at the air–sea interface; time variations of the oceanic evaporation and sensible heat flux are greater than expected. Using spectrum analysis, the occurrence of a 5-year periodicity in equatorial rainfall of the Pacific and Indonesia is demonstrated, together with a marked phase shift along the NE coast of New Guinea.

1 Introduction

Investigations of time-dependent correlations between large-scale circulation anomalies have recently aroused much interest especially after the most recent short-lived but drastic El Niño-episode in the equatorial Pacific (Ramage, 1975), which occurred simultaneously with the peak of the Sahel drought, with a severe deficiency of monsoon rains in the Indian subcontinent and with an exceptional drought in the European area of the Soviet Union. Altogether, these circulation anomalies caused a drop of the world's cereal production by about 6 percent, cutting the world reserves to one third, and triggered social unrest and even revolution (Ethiopia) in some developing countries. A preliminary survey (Fig. 1, Flohn, 1974) suggested a nearly simultaneous occurrence of such anomalies in different parts of the Tropics, indicating some kind of time-dependent zonal circulation as described by J. Bjerknes (1969) as the "Walker Circulation".

Half a century ago, Walker (1923) developed some ideas on the physical mechanism of his "Southern Oscillation", based mainly on the slow transport of ocean temperature anomalies in a zonal direction. This idea, however, was

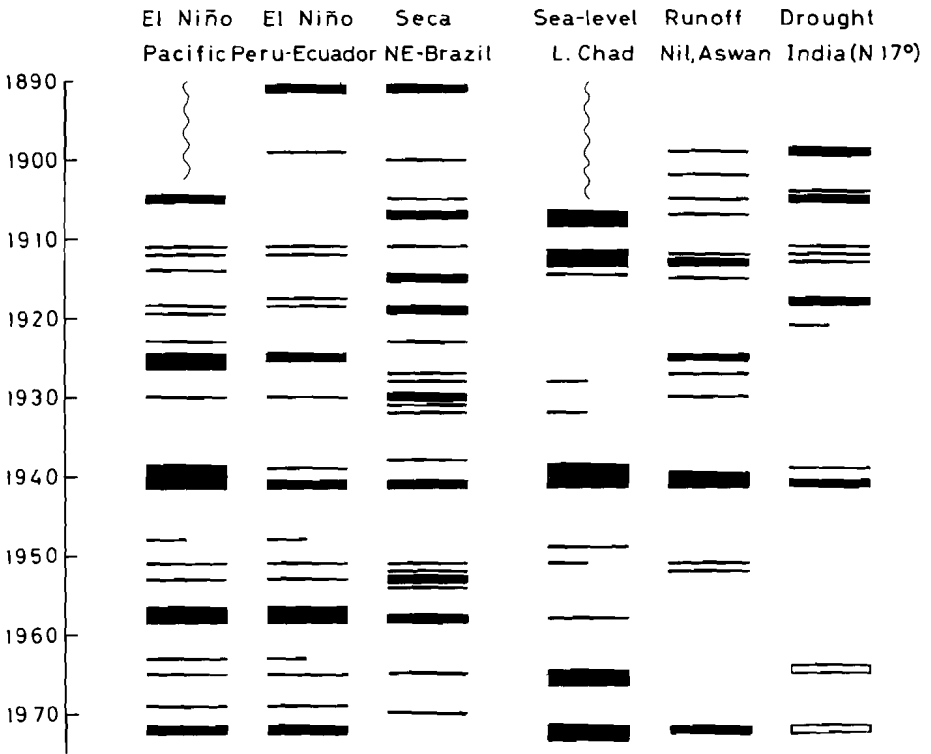|	El Niño Pacific	El Niño Peru-Ecuador	Seca NE-Brazil	Sea-level L. Chad	Runoff Nil, Aswan	Drought India (N 17°)

Fig. 1   Recent climatic anomalies in six tropical areas (preliminary survey).

not consistent with the facts now emerging from broader studies (Berlage, Troup, Namias and others). It was particularly J. Bjerknes (1964) – quoting some earlier results of Arkhipova – who stressed the importance of the oceanic heat budget and its time fluctuations.

My own interest in this matter was aroused by the Atlas of monthly anomalies of wind, water temperature and cloudiness along the shipping route Europe–South America (Bullig, 1954), covering a period of 25 years interrupted by the first World War. Using these data, Eickermann and Flohn (1962) investigated the teleconnections between the south-equatorial rainfall anomalies along the West African coast and those of drought-ridden and overpopulated Northeast Brazil. Here the phenomenon of coastal and equatorial upwelling could not be overlooked, being analogous to the more extended anomalies in the eastern and central Pacific. This phenomenon was studied along the coasts of Ecuador and Peru (Flohn and Hinkelmann, 1952; Schütte, 1969) as well as over the equatorial Pacific (Doberitz et alii, 1967; Doberitz, 1968); a final investigation found a negative correlation between Atlantic and Pacific (Doberitz, 1969).

2 Tilted circulation cells

The coincidence of circulation anomalies in different parts of the globe presents a great challenge for climatologists. A physical interpretation of such coinci-

Climatic Teleconnections with the Equatorial Pacific   97

dences has been given in terms of a meridional shift of large-scale climatic zones (Namias, 1972; Bryson, 1974). However, since the zonal extension of the equatorial belt is about 12 times longer than the meridional distance between the subtropical jet and the ITC, it is difficult to assume that meridional displacements of climatic zones occur independently of longitude. In the outer tropics (e.g. near 15 or 20° Lat.) and in the subtropics zonal temperature differences are not negligible when compared with the meridional differences. The phenomenon of diagonal cloud streets representing upper air troughs (Flohn, 1971) extending to the equator demonstrates the occurrence of large-scale variations in a zonal direction.

J. Bjerknes (1969) has first brought these zonal variations into the general concept of a zonally extended, thermally driven Walker circulation between an equatorial heat center – the "maritime continent" of Indonesia – and a cooling area at the eastern Pacific off the South American West Coast. Another smaller equatorial cell of this kind can be derived from a zonal cross-section of the vertically integrated heat budget W of an air column and of the satellite-derived planetary albedo a_p (Krueger 1970) between the heat center of the Amazon basin and the upwelling region off the West African coast. In opposite direction, a similar cell develops between this same cooling area and the "backbone of Africa" (Troll, 1973), maintained by the broad equatorial westerlies across this continent (Fig. 2). During northern summer, a similar circulation cell develops between the cool western Indian Ocean (including the coastal upwelling area off Somalia and SE-Arabia) and the areas with abundant rainfall of Southeast Asia.

The existence of the well-known mid-oceanic troughs, extending diagonally from the Subtropics to the ITC-region with a tilt of 50–60° Long. seems to be incompatible with the distinction of two perpendicular circulations, formally described, in a Cartesian coordinate system, as Hadley cell and Walker circulation. Krishnamurti (1971) has designed a system of quasistationary ultralong waves which can be interpreted as an interaction of both Hadley and Walker circulations. From this view-point we may visualize (Flohn, 1971) a system of tilted circulations within the tropical belt, which is also represented in the seasonal maps of the vertical wind speed at 500 mb, as derived from the continuity equation (Newell et al., 1974, Plate 9.2).

The heat sources are the areas of maximum rainfall in Indonesia, Central Africa and South America – in all cases supported by the orography and regional thermal circulations. In Indonesia it is the system of diurnal circulations driven in day-time by the highlands in the interior of the large islands, in nighttime by the unusually high water temperatures (28–29°) of the sea. Huge clusters with a diameter of more than 600 km develop each day: the area-averaged rainfall amount can be estimated to be near 220 cm yr^{-1}, equivalent to a release of latent heat of $\sim$170 W m^{-2}, much more than the net radiation near the surface. In the Amazon basin, recent investigations (Kreuels, Fraedrich and Ruprecht, 1975) have revealed, during southern summer, the existence of a quasi-permanent warm high-tropospheric anticyclone above a quasi-perma-
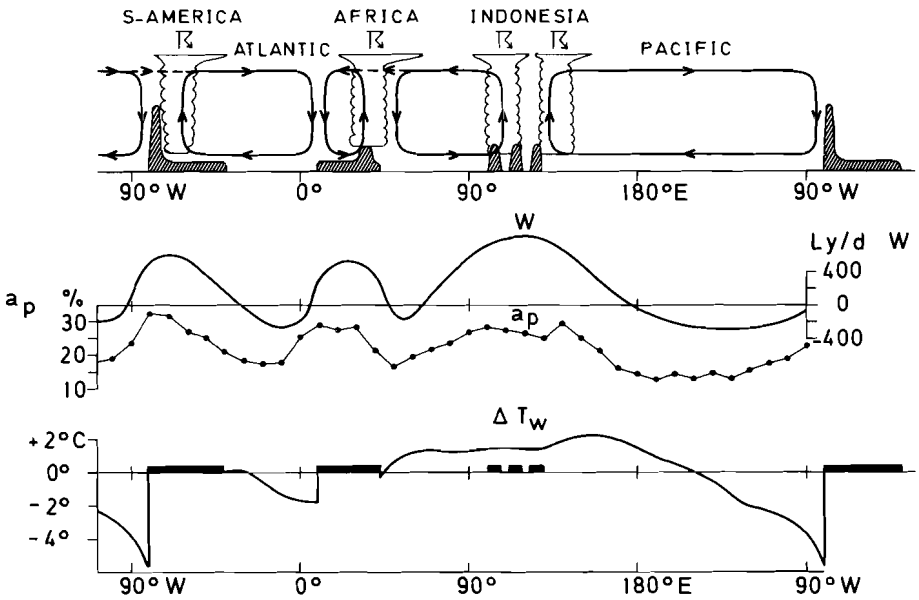
Fig. 2   Walker Circulation in equatorial latitudes, above; center: atmospheric heat budget
W and planetary albedo a_p (Krueger, 1970); bottom: sea surface temperature
anomalies (annual).

nent surface low. This situation appears as a homology to that of the Tibetan
High in northern summer, here concentrated at the NW flank of the elevated
altiplano of Peru-Bolivia in the eastern foothills of the Andes, where average
rainfall amounts 4–5 m yr^{-1} or more, equivalent to a latent heat release near
350 W m^{-2}. In southern winter, this system is shifted to the same foothills near
(and north of) the equator.

In the regions of upwelling cool water along the equator in the eastern Pacific,
about 30 percent of the net surface radiation is used for warming of upwelling
waters, evaporation is substantially reduced (Fig. 3) and – due to the down-
ward flux of sensible heat – large-scale convection is suppressed.

Upwelling is especially intense in the coastal regions of Peru and Angola,
in both cases concentrated between Lat. 5° and 20°S, where fog and low-level
stratus clouds add to the deficit of the heat budget. North of the ITC a similar
Walker circulation may exist, during northern summer, between the Cb con-
vection of the central and western Pacific and the large regions of upwelling
cool waters off California.

Because of this general pattern, where cooling is situated about 15° Lat.
polewards of heating a system of tilted thermal circulations develops, driven
by the isobaric temperature gradients between the rising unmixed air in the
hot towers of orographically triggered cumulonimbus clusters and the subsiding
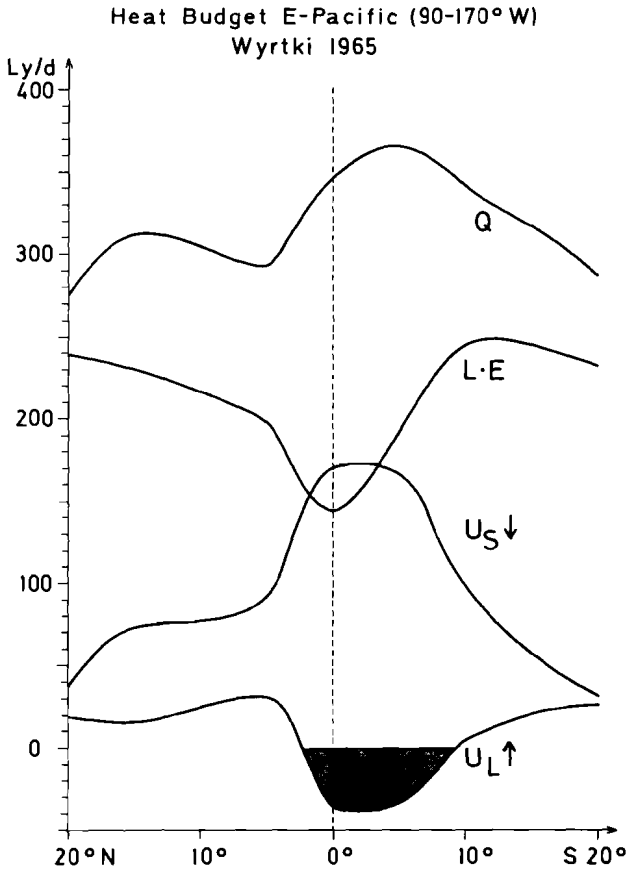air above the cool upwelling waters.

Climatic Teleconnections with the Equatorial Pacific   99

Fig. 3 Heat budget averages for the eastern Pacific (90–170°W, data after Wyrtki, 1965). Q = net radiation, LE = evaporation, U_s = heat flux into the sea, U_L (= H) = sensible heat flux into the air. 100 Ly d^{-1} = 48.5 W m^{-2}.

During northern summer, the large-scale temperature difference between the heated vast continental area between West Africa and South China, extending along 20°N over 140° of Longitude, and the relatively cool Pacific leads to two contrasting wind systems: the classical Trades above the Pacific and the Monsoon system, with a Tropical Easterly Jet above and Westerlies below. In the Monsoon system a meridionally displaced Hadley cell, east of India, is opposed to an Anti-Hadley cell above Africa, with rising cool equatorial air and subsiding warm air above the Sahara (Flohn, 1964). The meridional mass circulation in both Monsoon cells is estimated to be 100–180 kg cm^{-1} s^{-1}, in contrast to the oceanic Hadley cell on the order of 30–40 kg cm^{-1} s^{-1}. According to Newell *et al.* (1974, Fig. 9.3 and 9.5) the intensity of the zonal "Walker" mass circulation along the equator (taken as representative for ±10° Lat. at both sides) is on the order of 10 ± 5 kg cm^{-1} s^{-1}, with a maximum (during northern summer) in the eastern Indian Ocean near 90°E.

3 Air–Sea coupling

The purpose of teleconnection studies is now to reveal the space and time correlations between these different cells. The role of such investigations has been proved by the pressure correlations derived by Berlage (1966, cf. Newell, 1974, Plate 9.11). Our own contributions were mainly restricted to rainfall – this highly variable parameter being most essential within the Tropics.

While earlier investigations stressed the horizontal oceanic advection as driving agent, Doberitz, Flohn and Schütte (1967) and Doberitz (1968) demonstrated a near coincidence between the anomalies along the Peruvian coast and in the equatorial Pacific from the Galapagos to beyond the date-line. Regarding the red part of the spectrum (i.e. frequencies below 1 cycle per year) alone, the phase differences were surprisingly small in the zonal direction, but much larger and more systematic in a meridional direction, indicating a gradual spreading of the effect from the equator to the south with a speed near 10 cm s^{-1}, while at the northern side no data were available. The region of maximum coherency coincides with a disappearing annual cycle, with highest standard deviation and with highest persistency. In some contrast to Ramage's view (1975, p. 239), there exists a significant positive correlation between simultaneous monthly anomalies of rainfall and water temperature (Flohn, 1972), indicating a correlation between sensible heat flux and convective activity. Such positive correlations have also been demonstrated by Allison et al. (1971) and by White and Walker (1973). Furthermore, J. Bjerknes (1974) has shown a strong negative correlation between the intensity of the surface easterlies and the sea surface temperatures at Canton Island, indicating a direct forcing of the helical pumping of cold deep water to the surface near the equator by increasing wind drag. These results have been interpreted by an empirical model (Flohn, 1973), in which the normal Ekman-circulation in the upper oceanic mixing layer, favouring upwelling and suppressing convection along the equator, is in certain anomalous periods reverted, producing downwelling warm water and Cb convection extending to the equator. The relatively short times of transition between two quasi-stationary opposing states seem to indicate a kind of vacillation or flip-flop mechanism. However, maps of water temperature in Niño and non-Niño years (cf. Ramage, 1975, Fig. 6–8) both show a pattern of upwelling slightly south of the equator, only in a varying degree.

If these maps are truly representative, the reverted model of equatorial downwelling (Flohn, 1973) is partly inconsistent with the facts, and we observe only two states of upwelling of different intensity and position, probably correlated with the varying intensity of the trades and the subtropical anticyclone of the eastern South Pacific (Namias, 1973). On the other hand, another possibility of a flip-flop mechanism should also be considered: with a minor horizontal temperature gradient the flux of sensible heat between sea and air can remain positive, thus triggering convective activity near the equator. When the gradient becomes greater than a given threshold (depending on air temperature and wind component perpendicular to the isotherms), the sensible heat flux becomes negative resulting in a sudden complete suppression of Cb convection and shower activity.

Any interpretation of the upwelling phenomenon near the equator has to include also the fact, that the minimum temperature does not occur at the equator itself, but at about Lat. 2–3 °S. This is certainly true for the Atlantic (Henning, see Flohn, 1972), where the data had been collected in 2° intervals, and where the temperature difference sea-air reaches a minimum near 3 °S (Fig. 4). These facts are inconsistent with any simple model of the Ekman-drift diverging at the equator only because of the opposite sign of the Coriolis Parameter f on both sides of the equator. However, a more elaborate model taking into account the curvature of streamlines and the decrease of speed when approaching the equator may give a more realistic interpretation. The general relations between wind-field and Ekman-Drift near the equator have been discussed qualitatively (Flohn, 1972). It should also be investigated how far the oceanic current system, especially the Cromwell Undercurrent, may perhaps respond to far distant factors, producing active uplift or downwarping.

The average meridional variation of the surface heat budget components (Fig. 3) allows a conservative estimate of the variation of the fluxes of latent and sensible heat between normal and El Niño years (with positive sensible heat flux and a significant increase of the evaporation). While Rowntree's model (1972) gives an increase of evaporation of 55 percent for the zone 0–6°N, our estimate gives a minimum of +25%. As a consequence of this energy increase, the intensity of the subtropical jet has been more than doubled during the "warm" year 1972 (Table 1).

TABLE 1.   200 mb vector wind speed, average for June and July.

Station	1971	1972	1973
Lihue (Kauai)	12.0	29.2	12.6 ms^{-1}
Hilo (Hawaii)	16.5	27.2	14.2 ms^{-1}

This increase has been predicted by Rowntree's model, in spite of its somewhat unrealistic assumption of an equatorial "wall".

4 Temporal Variability

The interdiurnal and interannual variability of both sensible (H) and latent (LE) heat fluxes above the oceans is much greater than hitherto suspected. Because of the weak but not negligible correlation between wind speed and thermal stability $(T_s\text{-}T_a)$ or saturation deficit $(q_s\text{-}q_a)$ – see Kraus-Morrison (1966) – daily values of LE at the equator can vary between 63 and 233 W m^{-2} within a few days (Augstein, 1972). Even half year averages at a mid-ocean Weather Ship (C) can vary by ±25–30% (Table 2). The same is true for individual years in the tropical Atlantic, averaged between 10°N and 10°S (Henning, unpublished). In a remarkable coincidence the decadal averages at Weather Ships C (central N-Atlantic) and N (subtropical Pacific) for 1961–70 are 15–30% lower, both for H and LE, than those for 1951–1960. In the Pacific, this coincides with the weaker intensity of the Aleutian Low after 1963
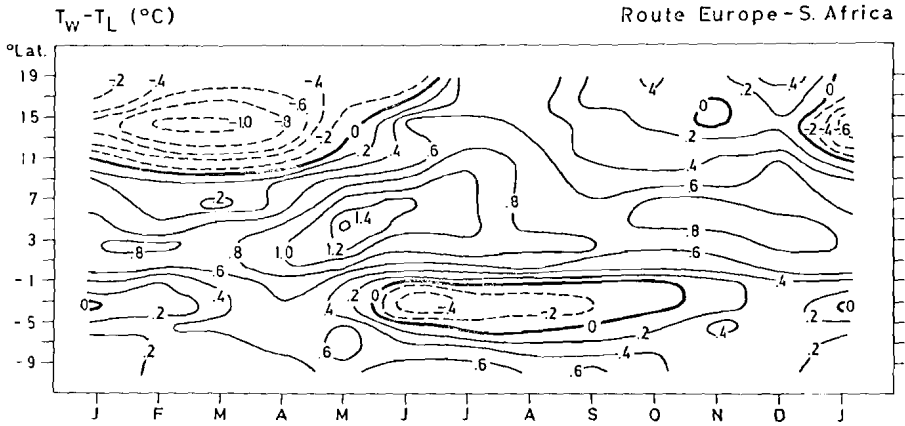
Hermann Flohn and Heribert Fleer

Fig. 4   Isopleths of temperature difference sea (T_W) – air (T_L) along the Atlantic shipping route Europe-South Africa (after D. Henning, cf. Flohn 1972).

TABLE 2.   Fluxes of sensible (H) and latent (LE) heat at Weather Ships C (53°N, 35°W) and N (30°N, 140°W).

	H	LE	$LE + H$
Atlantic Ship C, Winter (*October–March*)			
Average 1951/2–1972/3	22.3	151.0	173.3 W m^{-2}
Maximum	38.8	192.3	213.1
Minimum	5.1	118.1	134.2
Interannual Variability	9.1	23.1	23.0
Average 1951/2–1960/1	24.1	161.1	185.2
Average 1961/2–1970/1	18.6	138.5	157.1
Difference	– 22	– 14	– 15%
Pacific Ship N, Year			
Average 1954–60	15	126	141 W m^{-2}
Average 1961–70	10.5	103	113.5
Difference	– 30	– 18	– 20%

(White and Walker, 1973); but it seems to be at variance with the significant cooling of the Arctic troposphere since that time, especially with the extension of the summer-time cold vortex (Fig. 5).

Such large variations lead to the growing conviction (Namias, 1968, 1973) that the thermal (and dynamical) interaction between ocean and atmosphere – including the interaction with Arctic and Antarctic drift-ice – contains the key to any reasonable solution of the long-range (and climatic) forecasting problem. The small values of H should not be underrated: the horizontal variation of H triggers the initiation of thermal circulations, while its sign controls occurrence or non-occurrence of convection. The intensity of both processes, however, varies with latent heat released by precipitation (LP), mainly produced by dynamical parameters such as CISK. Oceanic evaporation apparently is not constant with time, perhaps not even on a global scale.

Climatic Teleconnections with the Equatorial Pacific   103
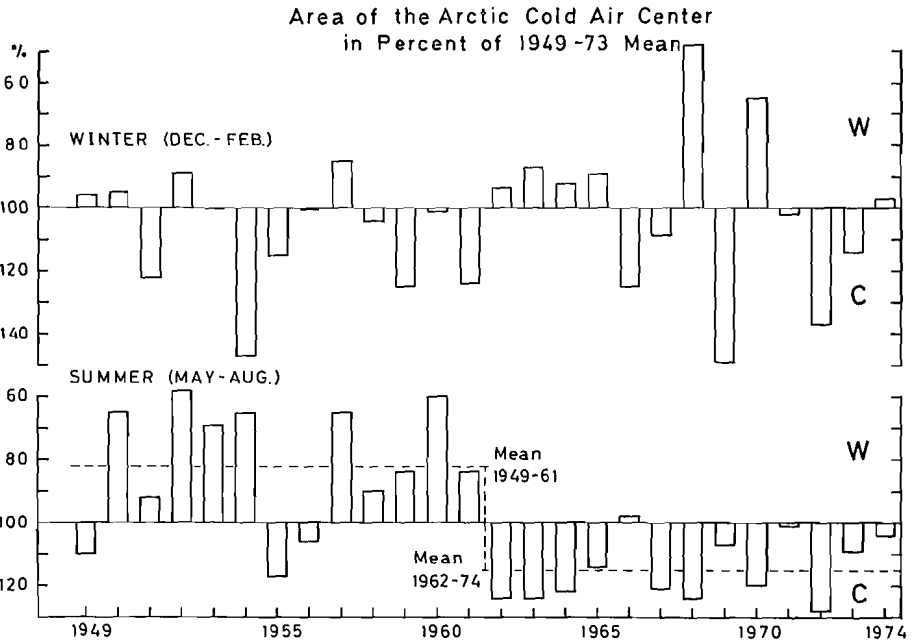
Fig. 5   Area of the Arctic Cold Center (thickness 500/1000 mb layer) in percent of the
1949–73 average (Flohn and Rodewald, 1975).

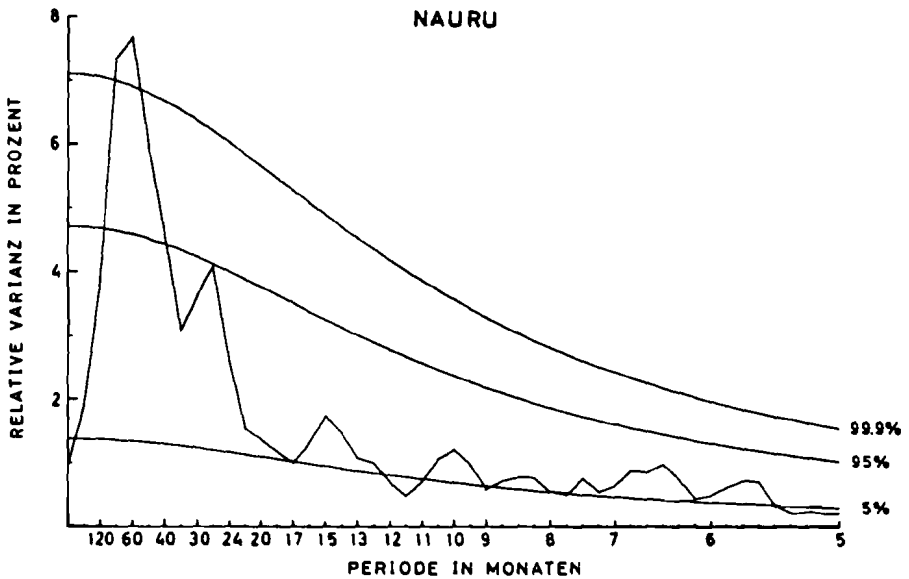Fig. 6   Power Spectrum of Nauru rainfall anomalies (partly reconstructed, annual march
removed, Fleer, 1975).

Hermann Flohn and Heribert Fleer

5 Spectral and cross-spectral analyses

In extension of the investigations carried out by Schütte and Doberitz, recent studies (Fleer, 1975) deal with the teleconnections of rainfall anomalies between Indonesia, northern Australia and the equatorial Pacific, using mainly records of about 60–70 years until 1972, with a few interruptions. On the basis of the existing strong correlations, the gaps of the very long record of Nauru (starting 1892) could be filled using the simultaneous anomalies of nearby Ocean Island and of far-distant Fanning, thus providing a representative 82 year-record. After removal of the annual cycle, spectrum analysis shows a typical red spectrum, with a significant peak at 4–5 years (Fig. 6), while the
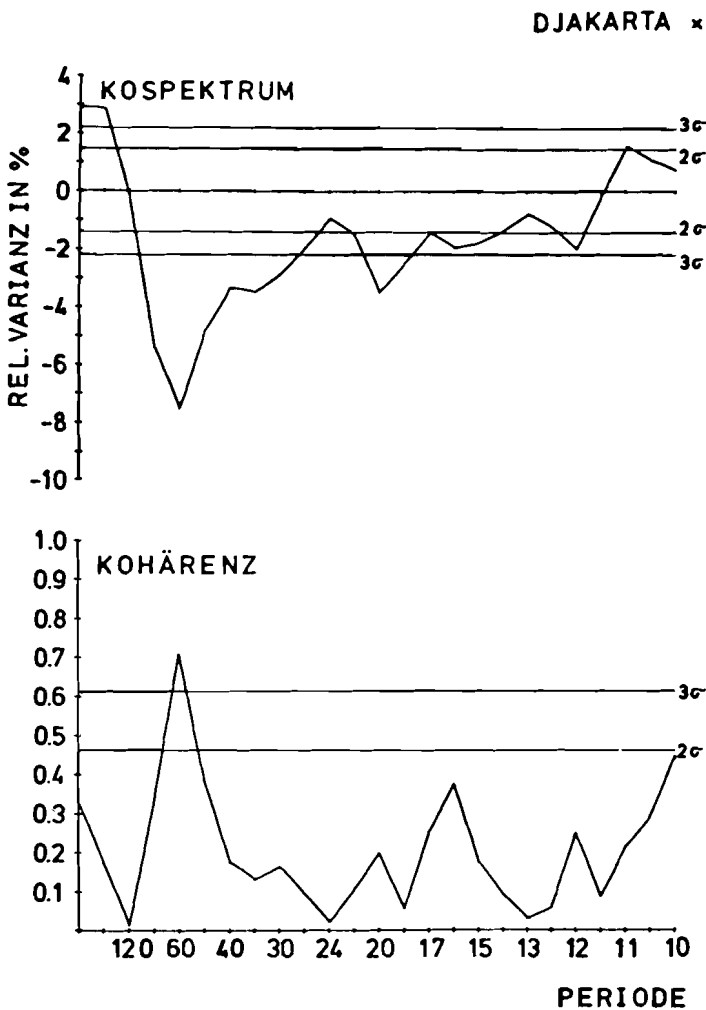

Fig. 7   Co-spectrum and Coherency between Djakarta and Fanning Isl. rainfall (Fleer, 1975), period in months.

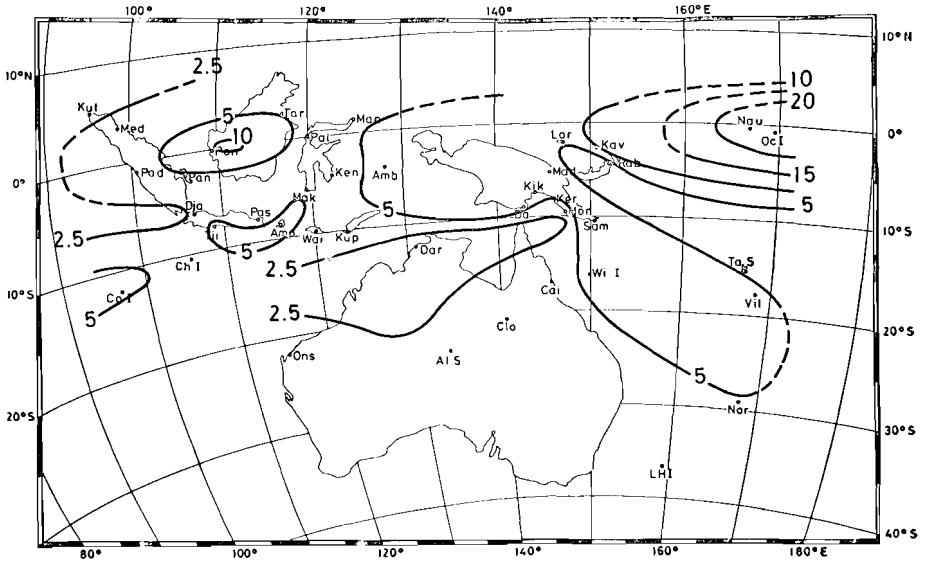Climatic Teleconnections with the Equatorial Pacific   105

Fig. 8 Contribution of the 4–6.7 year cycle to the total variance of rainfall (Fleer, 1975).

autocorrelation remains significant up to 6 months. The distribution of spectral types resembles that in the Pacific (Doberitz, 1968): a red spectrum type, but with a negligible contribution of the annual cycle, extends along the equator to Admiralty Islands, while a transitional spectrum type covers large parts of Indonesia.

The most interesting results are furnished by cross-spectrum analysis. Here even far distant stations, such as Djakarta versus Fanning Island (more than 10,000 km apart), show a marked coherency (= frequency-dependent correlation coefficient r^2) at a wave length of 5 years (Fig. 7), with comparatively minor phase differences. Wavelengths near 5 years are much better represented (Fig. 8) than those between 24 and 30 months. The quasi-biennial wave plays here, right at the equator, only a minor role. Most striking is the distribution of the coherency of the 5-year-wave: along the north coast of New Guinea, a marked shift separates two internally consistent areas with opposite sign, i.e. in opposite phase (Fig. 9).

This discontinuity coincides, to some extent, with Berlage's (1966) and Troup's (1965) pressure correlations of the Southern Oscillation. It should also be mentioned that a two-dimensional tropical circulation model (Webster, 1973, Fig. 12), heated by precipitation and by external forces, yields seasonal anomalies of the 250 mb geopotential, which also resemble rather accurately this pattern. If this is more than a coincidence, we may interpret the mechanism of the low-frequency part of the "Southern Oscillation" as related to the varying intensity of rainfall heating in the two contrasting areas: equatorial Pacific
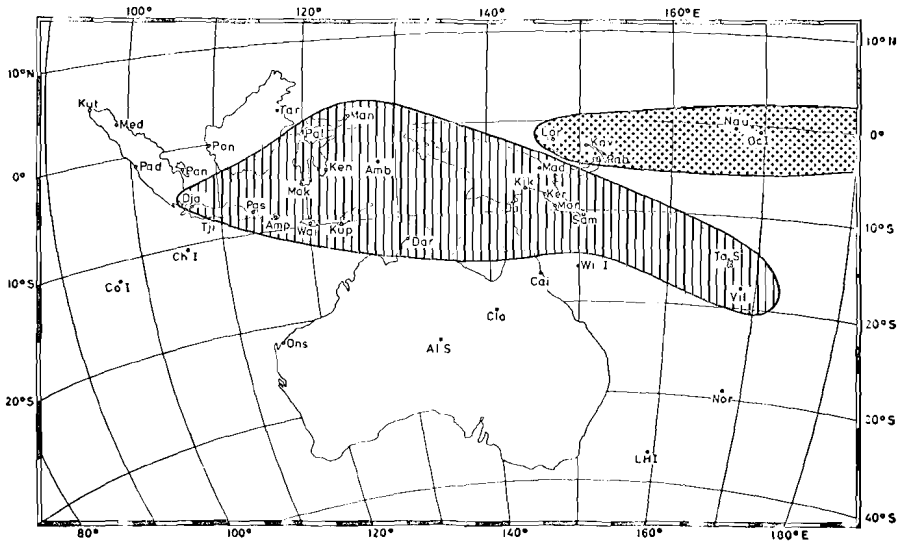
Fig. 9   Sign of the coherency of ~5 year cycles (reference station Djakarta, Fleer, 1975).

versus Indonesian islands – which does not, however, present a physical cause for a cycle of about 5 years. Between Indonesia and the Indo-Pakistan subcontinent a positive correlation seems to exist, at least for pressure (Berlage, 1966). The preliminary survey of anomaly years in the Tropics (Fig. 1) indicates also a significant negative correlation between the Indian Monsoon and the rainfall at the equatorial Pacific, i.e. the intensity of the N-Pacific Hadley cell.

Spectrum analysis verifies the result of Berlage and others, that the occurrence of anomalies is not strictly periodic: instead it is quasiperiodic, with preferred frequencies between 3 and 7 years, while the biennial period contributes only a minor part of the total variance. In some of the climatic parameters of this area, a 5-year period had been found earlier by Walker, Troup, Berlage and also by Kidson (1975), but in many cases only for a restricted time. Preliminary filter analysis has verified such time variations in the long records of Djakarta and Nauru. Outside of the Tropics, some examples of a significant 5-year peak have been found in 100 year temperature and precipitation records (Schönwiese, 1974), for example temperature at Uppsala, Helsinki, precipitation at Frankfurt/M., New York, Adelaide, Bombay. But at even more other stations any peak at this part of the spectrum is lacking and no internally consistent pattern could be found. The powerful discriminating tool of cross-spectrum analysis has not yet been applied; it would be interesting also to investigate the coherency with the half sun-spot cycle frequently used by F. Baur (1949) and others.

In addition to this apparent see-saw relation between Indian and Pacific Ocean another phase shift has been observed near South America (Berlage, 1966; Doberitz, 1969), with a negative correlation between the regions of

wide-spread near-simultaneous anomalies in the equatorial Pacific and in the equatorial Atlantic. Here the zero-correlation isopleth runs right across South America; a small center of negative correlations covers also the tropical South Atlantic. Further studies on the rainfall anomalies of Africa are under way: Berlage's maps seem to indicate that in this time-scale the zonal correlations between the tropical anomaly centers are much stronger than the meridional teleconnections with the extratropical westerlies. This is also confirmed by the decoupling of a correlation between the Aleutian Low and equatorial rainfall (White and Walker, 1973). To understand this mechanism, we need more data about the time variability of the sea-air fluxes and of rainfall, which apparently control a quite effective mechanism responsible for large-scale quasi-persistent anomalies of the atmospheric circulation (Namais, 1973).

6 Conclusion

Parallel to investigations with sufficiently realistic numerical models, taking into account the large-scale heat budget variations, we should look much more carefully into the existing records, using them to look into the solutions of the set of equations, which nature itself has provided. Much data are "successfully hidden" in the files of meteorological and other services; their cooperation in most cases should be gratefully acknowledged. Studies of this kind not only can give valuable hints to the understanding of the physical mechanism of the climatic system; they supply also the background, against which numerical climatic models can be checked.

References

ALLISON, L.J. *et alii*, 1971: Air-Sea Interaction in the tropical Pacific Ocean. Goddard Space Flight Center, Report X-651-71-191.

AUGSTEIN, E., 1972: Untersuchungen zur Struktur und zum Energiehaushalt der Passatgrundschicht. Ber. Inst. Radiometeor. Marit. Meteor. Hamburg 19.

BAUR, F., 1949: Die doppelte Schwankung der atmosphärischen Zirkulation in der gemässigten Zone innerhalb des Sonnenfleckenzyklus. *Meteor. Rundsch.* **2,** 10–15.

BERLAGE, H.P., 1966: The Southern Oscillation and world weather. *Med. Verh. Kon. Ned. Met. Inst.* **88.**

BJERKNES, J., 1964: Atlantic air-sea interaction. *Advances in Geophysics,* **10,** 1–82.

BJERKNES, J., 1969: Atmospheric teleconnections from the equatorial Pacific. *Mon. Wea. Rev.,* **97,** 163–172.

BJERKNES, J., 1974: A study of Canton Island winds. *Bonner Meteor. Abhandl.,* **17,** 297–301.

BRYSON, R.A., 1974: A Perspective on Climatic Change. *Science,* **184,** 753–760.

BULLIG, H., 1954: *Atlas der Monatswerte von Wassertemperatur, Wind und Bewölkung auf dem Seeweg Europa-Südamerika.* Dt. Wetterdienst, Einzelveröff. Seewetteramt Hamburg 5.

CAVIEDES, C.N., 1973: Secas and El Niño: two simultaneous climatical hazards in South America. Proc. Assoc. Amer. Geographers, **5,** 44–49.

DOBERITZ, R., H. FLOHN and K. SCHÜTTE, 1967: Statistical investigations of the climatic anomalies of the equatorial Pacific. *Bonner Meteor. Abhandl.,* **7.**

DOBERITZ, R., 1968: Kohärenzanalyse von Niederschlag und Wassertemperatur im tropischen Pazifischen Ozean. *Ber. Dr. Wetterdienst,* **112;** cf. also *Bonner Meteor. Abhandl.,* **8.**

DOBERITZ, R., 1969: Cross spectrum and filter analysis of monthly rainfall and

wind data in the tropical Atlantic region. *Bonner Meteor. Abhandl.*, **11**.

EICKERMANN, W. and H. FLOHN, 1962: Witterungszusammenhänge über dem äquatorialen Südatlantik. *Bonner Meteor. Abhandl.*, **1**.

FLEER, H., 1975: Spektrum- und Kreuz-spektrumanalyse von Niederschlagsreihen aus Indonesien, Australien und West-pazifik. Diploma Thesis, Universität Bonn.

FLOHN, H. and K. HINKELMANN, 1952: Äquatoriale Zirkulationsanomalien und ihre klimatische Auswirkung. *Ber. Dt. Wetterdienst US-Zone*, **42**, 114–121.

FLOHN, H., 1964: Investigations on the Tropical Easterly Jet. *Bonner Meteor. Abhandl.*, **4**.

FLOHN, H., 1971: Tropical Circulation Patterns. *Bonner Meteor. Abhandl.*, **15**, and in: *Physical and Dynamical Climatology*. WMO-Symposium Leningrad, 1971 (printed 1974), 180–198.

FLOHN, H., 1972: Investigations of equatorial upwelling and its climatic role. In: A.L. Gordon, *Studies in Physical Oceanography Vol. 1*, New York, 93–102.

FLOHN, H., 1973: Remarks on climatic intransitivity and the 1972 Pacific anomaly. *Atmosphere*, **11**, 134–140.

FLOHN, H., 1974: Instabilität und anthropogene Modifikation des Klimas. *Ann. Meteor. N.F.* **9**, 25–31.

FLOHN, H., 1975: History and intransitivity of climate. WMO-GARP-Publication Series 16, p. 106–118.

FLOHN, H. and M. RODEWALD, 1975: Beiträge zum Problem der aktuellen Klima-Variationen. *Beilage zur Berliner Wetterkarte 89/75*, 13 S.

KREUELS, R., K. FRAEDRICH and E. RUPRECHT, 1975: An aerological climatology of South America. *Meteor. Rundsch.*, **28**, 17–24.

KIDSON, J.W., 1975: Tropical Eigenvector Analysis and the Southern Oscillation. *Mon. Wea. Rev.*, **103**, 187–196.

KRAUS, E.B. and R.E. MORRISON, 1966: Local interactions between the sea and the air at monthly and annual time-scales. *Quart. J. Roy. Meteor. Soc.*, **92**, 114–127.

KRISHNAMURTI, T.N., 1971: Tropical east-west circulation during the northern summer. *J. Atmos. Sci.*, **28**, 1117–1133.

KRUEGER, A.F., 1970: The zonal variation of cloudiness and convection over the Tropics. Proc. Symp. Trop. Meteor. Honolulu, Hawaii, I III.

NAMIAS, J., 1968: Long-range weather forecasting – history, current status and outlook. *Bull. Am. Meteor. Soc.*, **49**, 348–470.

NAMIAS, J., 1972: Influence of northern hemisphere circulation on drought in northeast Brazil. *Tellus*, **24**, 336–343.

NAMIAS, J., 1973: Collaboration of ocean and atmosphere in weather and climate. Proc. 9th Ann. Conf. Mar. Technol. Soc. 163–178.

NEWELL, R.W. *et alii*, 1974: *The general circulation of the tropical atmosphere and interactions with extratropical latitudes, Vol. 2*, MIT-Press, 371 pp.

RAMAGE, C.S., 1975: Preliminary discussion of the meteorology of the 1972–73 El Niño. *Bull. Am. Meteor. Soc.*, **56**, 234–242.

ROWNTREE, P.R., 1972: The influence of Tropical East Pacific Ocean temperatures on the atmosphere. *Quart. J. Roy. Meteor. Soc.*, **98**, 290–321.

SCHÖNWIESE, CHR. D., 1974: Schwankungsklimatologie im Frequenz- und Zeitbereich. Diss. Univ. München, 139 S.

SCHÜTTE, K., 1969: Untersuchungen zur Meteorologie und Klimatologie des El Niño-Phänomens in Ecuador und Nordperu. *Bonner Meteor. Abhandl.*, **9**.

TROLL, C., 1974: Das "Backbone of Africa" und die afrikanische Hauptklimascheide. *Bonner Meteor. Abhandl.*, **17**, 209–222.

TROUP, A.J., 1965: The Southern Oscillation. *Quart. J. Roy. Meteor. Soc.*, **91**, 490–506.

WALKER, G.T., 1924: Correlation in seasonal variations of weather VIII; IX. Mem. India Meteor. Dept. 24, 75–131, 275–332.

WEBSTER, P.J., 1973: Temporal variation of the low-latitude zonal circulations. *Mon. Wea. Rev.*, **101**, 803–816.

WHITE, W.B. and A.E. WALKER, 1973: Meridional Atmospheric Teleconnections over the North Pacific from 1950 to 1972. *Mon. Wea. Rev.*, **101**, 817–822.

WYRTKI, K., 1965: The average annual heat balance of the North Pacific Ocean and its relation to ocean circulation. *J. Geophys. Res.*, **70**, 4547–4560.

Climatic Teleconnections with the Equatorial Pacific

Airflow from Mustard to Fallow

R.P. Angle

Alberta Environment, Edmonton, Alberta
[Manuscript received 10 March 1975; in revised form 15 September 1975]

ABSTRACT

Real terrain is complex and its effects on the atmosphere are not well understood. The two-dimensional change-of-roughness problem is investigated in an experimental study of airflow from mustard to fallow. The surface friction velocity is found to overshoot and return slowly to the equilibrium value. The wind profile in the modified region is more nearly logarithmic than the Peterson model predicts. The simple Elliot theory is in fair agreement with the wind profile data. Values for the ratio of the standard deviation of the vertical wind to the friction velocity reveal no variation with stability and are in close agreement with the value for laboratory flows. Values for the ratio of the standard deviation of the longitudinal wind component to the friction velocity are comparable to other recently determined atmospheric values and show a variation attributable to large-scale terrain properties.

1 Introduction

Micrometeorological theory, for the most part, has been developed on the assumption that the underlying surface is uniform and of unlimited extent. The 'homogeneous infinite plane' is an idealization to which natural terrain corresponds only in exceptional cases. On one scale or another the earth's surface is characterized by spatial changes in roughness, temperature and moisture. It is only recently that systematic study has been directed toward determining the effects of this "patchiness" on the vertical profiles and fluxes.

Knowledge about the response of flow properties to typical surface irregularities can be used in two important ways: (1) It will enable the experimentalist in the field to ascertain whether his measurements are, in fact, representative of the surrounding area. A rule for representative measurements can then be formed relating the maximum height of measurement to the fetch over the upwind surface (height-to-fetch ratio); (2) It will shed some light on the adequate representation of boundary layer effects in numerical forecasting and general circulation modelling. The surface is an important link in the energy exchange process, one familiar effect being airmass modification.

The simplest form of change is an abrupt transition from one uniform surface to a second uniform surface. Adjustment of the flow is intuitively expected to grow very much like the boundary layer on a flat plate. The effect of such discrete changes is often called the problem of the internal boundary layer. To

date the most progress has been made on the two-dimensional change of rough-ness problem. Numerous analytical and numerical solutions have been ad-vanced. These are reviewed in Plate (1971) and Angle (1973).

Three analytical solutions (Elliot, 1958; Panofsky and Townsend, 1964; Townsend, 1966, as revised by Blom and Wartena, 1969) and three numerical solutions (Taylor mixing-length, 1969; Glushko, presented in Taylor, 1972; Peterson, 1969, as modified slightly by Taylor, 1972) were examined in detail. The wind profiles predicted by the first five of these theories differ significantly only near the top of the internal boundary layer. The Peterson model, however, makes the unique prediction of an inflection point below the interface. All of the solutions differ considerably in the predicted shear stress distributions.

2 The micrometeorological experiment
a The Experimental Site
A site suitable for a change-of-roughness study must meet several requirements: (1) It must be level to avoid orographic effects; (2) It must be free of large obstacles that would disturb the flow; (3) There must be a long fetch across a uniform surface to ensure equilibrium of the flow; (4) There must be a step change to a second uniform surface in order to reproduce the two-dimensional situation of the theories.

After no little search a reasonably suitable site was located on the farm of Mr. Bill Perry near Chin, Alberta. A detailed map of the region is shown in Fig. 1. The section of land slopes downward to the north with a maximum relief of about twenty feet in a mile. The instrumentation was situated at the edge of a mustard field on a fairly level area about midway down the field (east-west slope about 5 ft/mile). A uniform fetch of at least 1/6 mile (268 m) across the mustard was available in westerly (prevailing) winds. With easterly winds a uniform fetch of at least 1/6 mile (268 m) was available across the adjoining fallow. The nearest buildings were at the farmyard over ½ mile away, and the nearest trees were over 1 mile away.

b Instrumentation
The main tower was erected just in from the edge of the mustard field with the booms extending outwards over the mustard. Mean wind speeds were measured at 1, 2, 4 and 8 m with four RIMCO-CSIRO sensitive cup impulse anemometers. The 0.5 m level could not be used because the mustard was some 55 cm high. The vertical wind was measured with a sonic anemometer mounted on the main tower at a height of 3.66 m. Heat fluxes were measured with a Fluxatron at the same height. Momentum flux was measured by the eddy correlation technique with a vane-type shear stress meter also at a height of 3.66 m. Unfortunately the vertical propeller ceased to operate when a severe gust snapped the perspex retaining screw. A portable mast was erected on the fallow with two RIMCO-CSIRO sensitive cup anemometers at heights of 1 m and 2 m. When downstream profiles were to be taken three of the anemometers from the main tower were removed and mounted on the mast.

fallow   wheat   mustard   fallow   barley
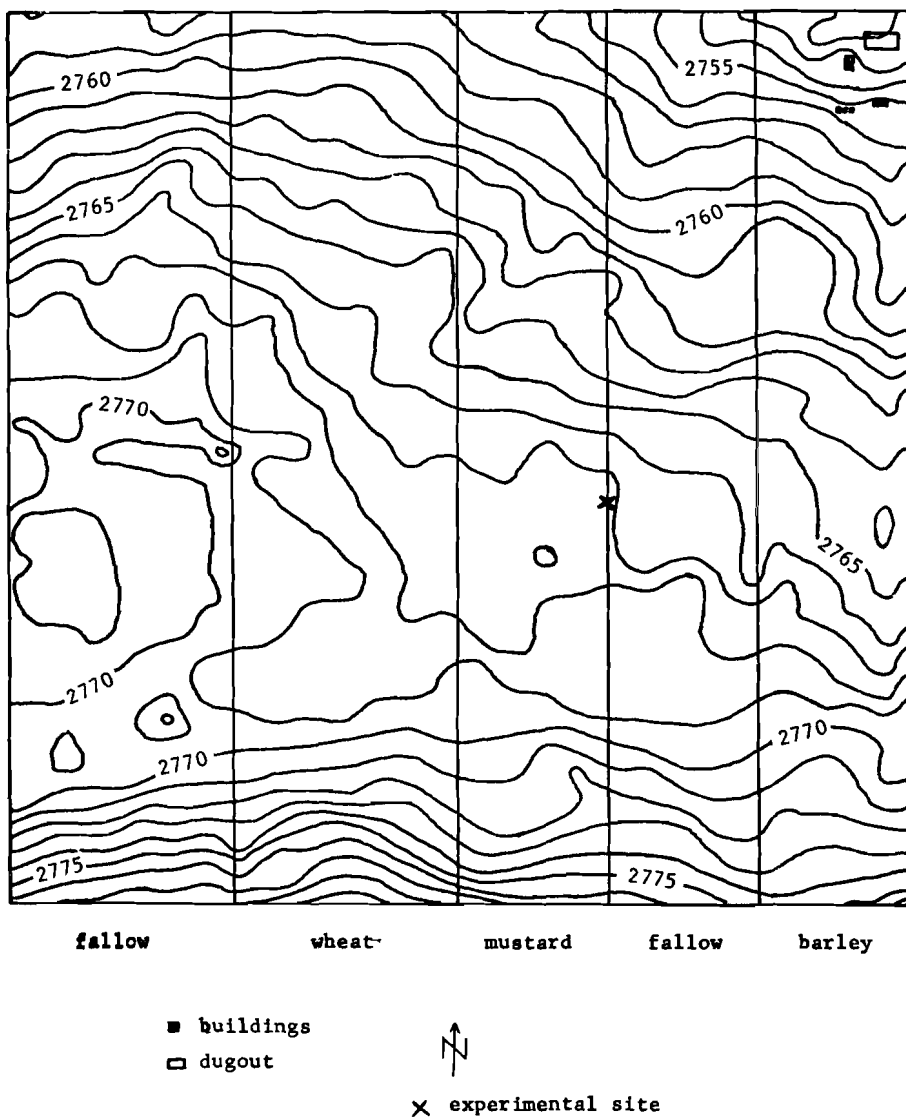
■ buildings
□ dugout

✕ experimental site

Fig. 1   One foot contours and agricultural use for the section of land on which the experimental site was located.

Data from the fast response instruments – the fluxatron, sonic anemometer, and shear stress meter – were recorded on tape by the multiplexing, digital conversion, minicomputer control system described by Honsaker, McDougall and Oracheski (1972). The mean wind was recorded by photographing electric impulse counters at 15 minute intervals. Temperature and dewpoint sensors were also mounted on the main tower. The former failed to function properly, although this was not discovered at the time. Hourly temperatures for the test days were obtained from the nearby Lethbridge airport.

3 Data analysis
a *Wind Profile Parameters*
In neutral conditions it is generally accepted that the wind profile is given by

$$u = (u_*/k) \ln z/z_0, z > z_0,$$

where u is the wind velocity at height z, u_* is the surface friction velocity, z_0 is the surface roughness, and k is von Karman's constant. When the roughness elements are large an additional parameter is often introduced so that the equation becomes

$$u = (u_*/k) \ln (z - d)/z_0, z > d + z_0,$$

where d is the zero-plane displacement. There has been considerable controversy over the exact role of this parameter. It has been interpreted variously as: (1) an empirical modification that provides a better fit for experimental data, (2) an allowance for the virtually stationary layer of air trapped within the roughness elements, (3) a datum level above which normal turbulent exchange takes place, (4) devoid of real physical significance because observed values are so variable and because the profile can be described just as well without it, (5) a shift in the origin of the z-axis because a vegetation cover produces an effective surface above the solid ground, (6) a corrective height increment between the mathematically defined zero plane and the arbitrary datum level from which an observer has measured anemometer heights, (7) a translation of the zero level for the vertical axis analogous to the displacement thickness in fluid mechanical boundary layer theory.

In non-neutral conditions it is generally accepted that the wind profile can be represented by

$$u = (u_*/k)[\ln (z - d)/z_0 - \psi]$$

where ψ is a function that gives the diabatic influence. For the unstable case, Paulson (1970) has derived the expression

$$\psi = 2 \ln \left[\frac{1 + r}{2}\right] + \ln \left[\frac{1 + r^2}{2}\right] - 2 \tan^{-1} r + \frac{\pi}{2}$$

where $r = (1 - \gamma z/L)^{1/4}$ and γ has the empirical value of 16. Given a set of wind observations at different levels and the corresponding heat flux, the three wind profile parameters can be evaluated using the method of least squares outlined by Stearns (1970).

The westerly winds of July 1, 1972 allowed twenty such computations to be made for the mustard based on hourly average windspeeds at four levels and the measured heat fluxes. Conditions varied from neutral to slightly unstable. The average value for the roughness of the mustard was found to be 12 cm with a standard deviation of 1.6 cm. The average value for the zero-plane displacement was 15 cm with a standard deviation of 3.7 cm.

The easterly winds of June 30, 1972 allowed a similar twenty computations to be made for the fallow using the hourly-average wind speeds at the two

levels of the portable mast and assuming d to be zero. Conditions were generally unstable. The average value for the roughness of the fallow was 1.0 cm with a standard deviation of 0.12 cm.

b *Comparisons*

Values for the displacement height are not plentiful in the literature, but some empirical formulas do exist. Sutton (1953) quoted Paeshke's result for dense crops that d is equal to the average of the measured heights of the roughness elements. Plate and Quraishi (1965) found for model crops in a wind tunnel that to a good approximation $d = h_c$ where h_c is the height of the crop. Taylor (1962) chose a value of $d = 1/5 \, h_c$ for long grass 50 cm high. Plate (1971) stated that in general d will differ from h_c when the density of the roughness elements is sparse. Geiger (1966) asserted that d is not equal to the average height of the vegetation surface and that only an examination of the wind profile can determine the value of d which will best satisfy the equation. Geiger also quoted some results of Deacon where a displacement of 25 cm was used for long grass 60–70 cm high, that is, $d = 2/5 \, h_c$. Monin and Yaglon (1971) took d to be zero for low vegetation and suggested the range $h_c/2 \leqslant d \leqslant h_c$ for high vegetation.

Geiger attributed this wide range of values to the high degree of pliability of plant stalks. Rauner (in Munn, 1966) found that as the wind speed increased over a forest the value of d decreased from $h_c/2$ to $h_c/4$.

The value obtained for the mustard was 15 cm and even though the wind speed at 1 m was fairly steady at 2 to 2.5 ms^{-1} the standard deviation was 4 cm. The ratio d/h_c for the mustard was 0.28. This was lower than most estimates, but higher than that of Taylor. A comparison of values computed from empirical formulas and those reported by various workers for similar crops is given in Table 1.

No micrometeorological studies appear to have been done over mustard as there are no published values for the roughness. Once again, however, there are a number of empirical formulas. Plate and Quraishi (1965) found that for crop-like elements in a wind tunnel $z_0 = 0.15 \, h_c$ in agreement with the field work of Paeshke (in Plate, 1971). According to Sellers (1965) a number of workers have used relationships of the form

$$\log z_0 = \log a + b \log h_c \text{ that is } z_0 = a \, h_c^b$$

where a and b are empirical constants. Values of b between 0.99 and 1.42 have been employed and values of $\log a$ ranging from -1.4 to -0.88. Plate (1971) objected to an equation of this form because it is not dimensionally consistent. Monin and Yaglom (1971) recommended that $h_c/10 \leqslant z_0 \leqslant h_c/5$, noting that the constant of proportionality is considerably greater than the value 1/30 for Nikuradse's sand roughness. They attributed the variability of estimates for both d and z_0 to the fact that both parameters depend on fairly fine details of surface structure. Natural vegetation, even of one type, is not likely to have identical structure in different places around the world.

R.P. Angle

TABLE 1. Some values for the zero-plane displacement of mustard 55 cm high and similar crops.

Value (cm)	Details	Source
15	Mustard 55 cm high	Observed at Chin
66	$d = h_c$, from models in a wind tunnel	Plate and Quraishi
27–55	$h_c/2 \leqslant d \leqslant h_c$	Monin and Yaglom
10	Grass 50 cm high	Taylor
25	Grass 60–70 cm high	Deacon
30	Grass 60–70 cm high	Calder
55	$d = h_c$, for field crops	Paeshke

TABLE 2. Some values for the roughness of mustard 55 cm high and similar crops.

Value (cm)	Details	Source
12	Mustard 55 cm high	Observed at Chin
8	$z_0 = 0.15\, h_c$, from models in a wind tunnel	Plate and Quraishi
22	Wheat 60 cm high	Penman and Long
11–15	Grass 60–70 cm high	Deacon
10.5	$z_0 = h_c^{1.2}/12$	Sellers
5.5–11	$h_c/10 \leqslant z_0 \leqslant h_c/5$	Monin and Yaglom
6–9	Long grass 60–70 cm high	Priestly
9	Thick grass up to 50 cm	Sutton
4–5	High grass, wheat	Hess
4–9	Long grass 60 cm high	Pasquill
14	Fully grown root crops	Pasquill
4–12	Tall grass, grain	Geiger
3	Grass 60–70 cm high	Calder
14	Roughness element formula ($s \sim 20\ cm^2$, $S \sim 40\ cm^2$)	Lettau

Lettau (1969) held that the use of only the height in a roughness formula is too restrictive and produces oversimplified results. The shape and spacing of the roughness elements must also be considered. On the basis of the bushel basket experiments he proposed the relation

$$z_0 = 0.5\ h_c\ s/S$$

where s is the silhouette area of the average obstacle, that is, the cross-sectional area 'seen' by the wind in an approach to a typical roughness element; S is the specific area or lot area, that is, the average area on the earth's surface occupied by a single roughness element. The factor 0.5 corresponds to the average drag coefficient of the characteristic element. Lettau considered estimates from this formula to be within $\pm 25\%$. Its validity is restricted to situations where $s < S$; otherwise serious overestimation occurs.

Table 2 gives a comparison of the value obtained for the mustard (12 cm) with values computed from the various formulas, and with values for similar crops reported in the literature. Table 3 shows values for the fallow.
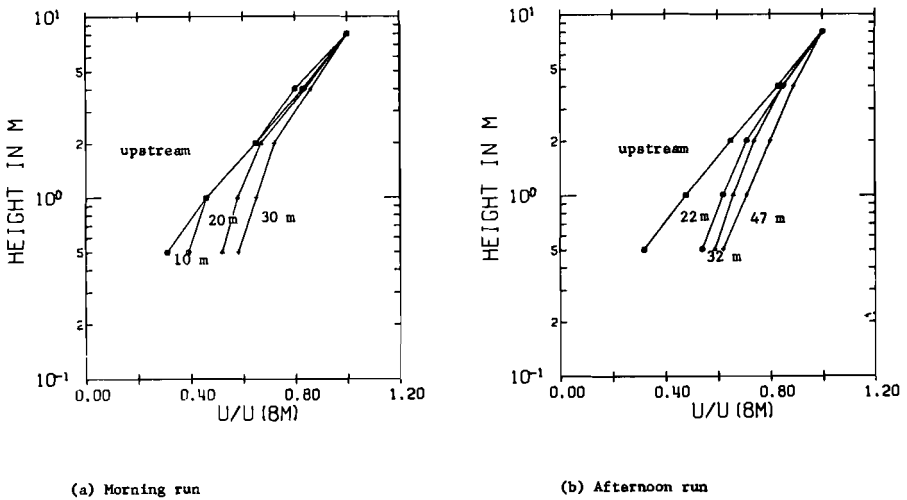
(a) Morning run   (b) Afternoon run

Fig. 2   Velocity profiles observed at Chin, Alberta.

c *The Downwind Profiles*

On the morning of July 1, 1972 near-neutral conditions prevailed as a result of heavy overnight cloud cover and moderate westerly winds. From 0640 to 0805 ten-minute wind profiles consisting of five levels up to eight metres were taken at distances of 10, 20 and 30 m downwind from the mustard-fallow boundary. Near-neutrality was confirmed by the heat flux measurements which gave a value for the Monin-Obukhov length of −770 m.

A second run was made in the afternoon of the same day from 1626 to 1712 MDT. The Monin-Obukhov length was −900 m, again very close to neutral. Unfortunately the wind had shifted to 320–330° so that a strictly two-dimensional situation was no longer present. Effective fetches of 22, 32 and 47 m were obtained.

The profiles observed during the morning and afternoon runs of July 1, 1972 are shown in Fig. 2. The velocities were scaled with respect to the wind at the highest observation level of 8 m, which is outside the modified region for these fetches according to most theories. The uppermost points of each profile lie on the line characteristic of the upstream flow, except the 4-m point at 10-m fetch which seems to be somewhat in error. The acceleration of the flow at increasing distances appears as a shift to higher speeds in the lower portion of the profiles. The number of points lying on the upstream profile decreases with distance.

The height of the internal boundary layer cannot be well defined by so few points, so direct comparison with predictions from the various theories has not been attempted. The surface friction velocities scaled with respect to the upwind value were computed from the 0.5-m wind speed by means of a drag coefficient. Assuming that the 0.5-m wind is in the portion of the profile characteristic of the new surface:
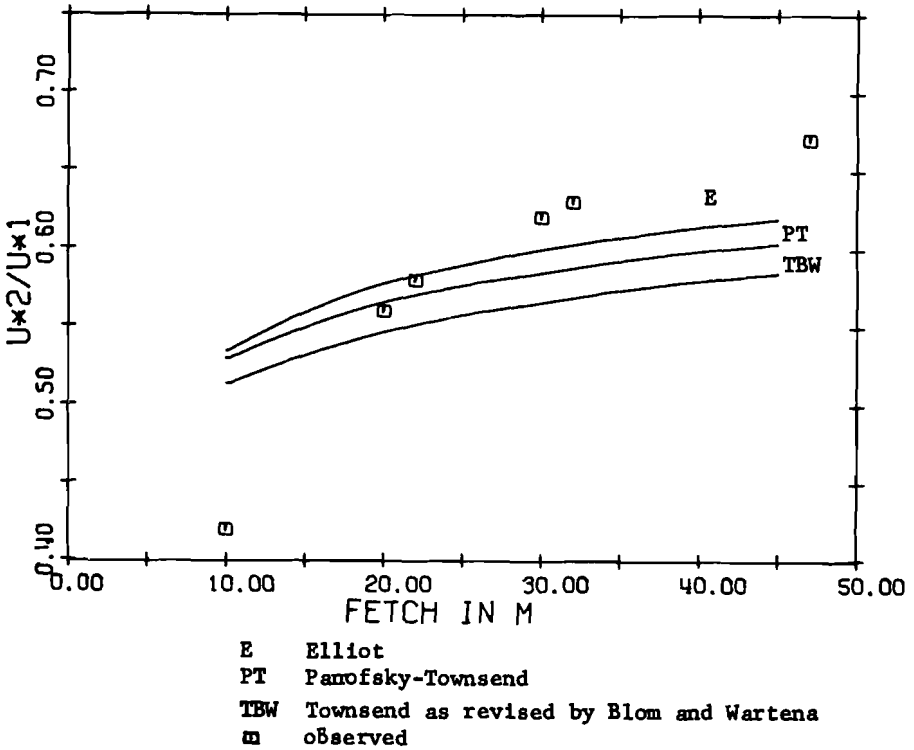
116   R.P. Angle

Fig. 3 Downwind variation of the surface friction velocity inferred from the wind at 0.5 m compared with three analytical solutions.

E	Elliot
PT	Panofsky-Townsend
TBW	Townsend as revised by Blom and Wartena
⊡	observed

$$u_{0.5m} = (u_{*\,2}/k) \ln (50/1)$$
$$u_{*\,2} = c_{d2}\, u_{0.5m} \text{ where } c_{d2} = k/\ln (50/1)$$

The wind at 8 m is characteristic of the upwind flow and assuming negligible streamline displacement

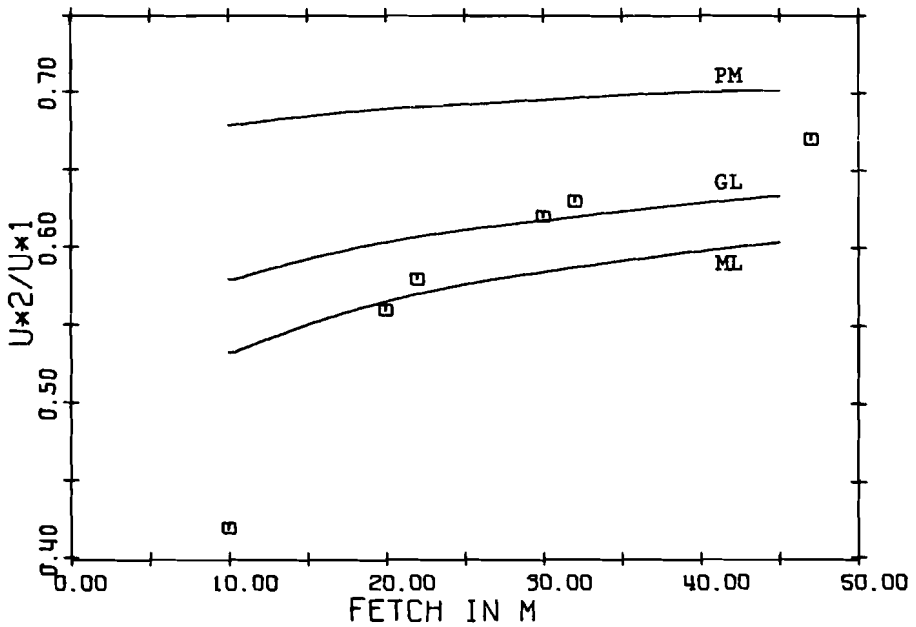$$u_{8m} = (u_{*\,1}/k) \ln (800/12).$$

With $u_{*\,1} = c_{d1}\, u_{8m}$ where $c_{d1} = k/\ln (800/12)$ it follows that

$$u_{*\,2}/u_{*\,1} = (c_{d1}/c_{d2})\, u_{0.5m}/u_{8m}.$$

Fig. 3 compares values of the friction velocity computed in this way with three analytical solutions. Fig. 4 does the same for three numerical solutions. The initial overshoot was greater and the recovery was rather more rapid than predicted by any of the theories. There is a suggestion that at larger fetches either the Glushko or Peterson model would provide a suitable description of the surface shear stress adjustment.

To facilitate direct comparison of the observed velocity profiles with the results of the various theories, a transformation was employed to scale the speeds with respect to the upstream friction velocity:

$$u/u_{*\,1} = u/u_{8m} \cdot u_{8m}/u_{*\,1}$$

Airflow from Mustard to Fallow   117

Fig. 4   Downwind variation of the surface friction velocity inferred from the wind at
0.5 m compared with three numerical solutions.

PM   modified Peterson
GL   Glushko
ML   mixing-length
☐   observed

TABLE 3.   Some values for the roughness of fallow and similar
terrain.

| Value (cm)	Details	Source
1.0	Fallow with some trash	Observed at Chin
2.1	Fallow field	Hess
0.6–2.0	Countryside, prairie	Geiger
0.2–2.5	Mown grass 1.5–4.5 cm	Priestly
0.7–2.3	Downland, thick grass up to 10 cm high	Sutton
0.5	Short grass	Calder
1.7	Grassy surface	Plate
2.1	Flat country	Plate

The first factor is the observed value and u_{8m}/u_{*1} can be calculated because the 8-m wind is characteristic of the upwind flow, that is

$$u_{8m}/u_{*1} = (1/k) \ln (800/12)$$

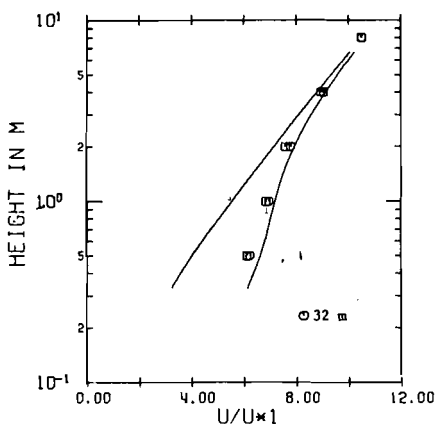118   R.P. Angle
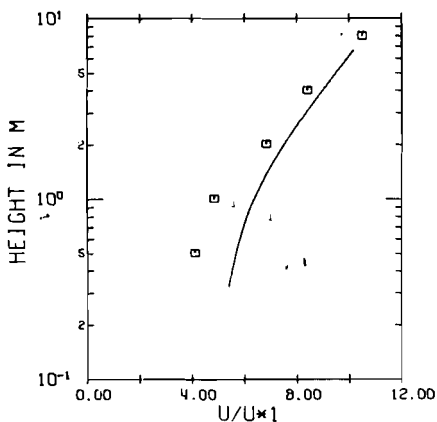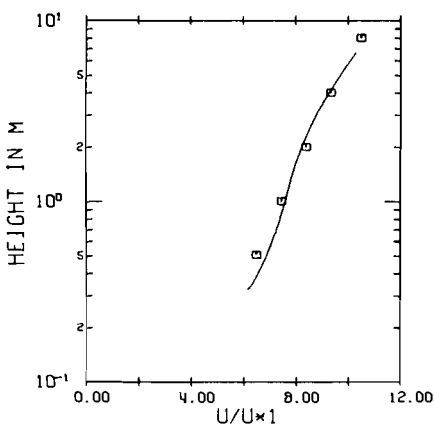
(a) Fetch 10 m
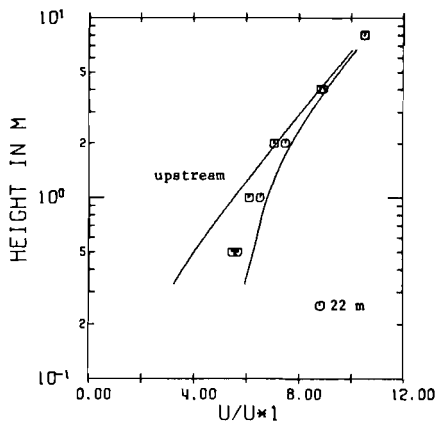
(b) Fetch 20 m

Fig. 5   Observed wind profiles compared with the modified Peterson model.

(a) Fetch 30 m

(b) Fetch 47 m

Fig. 6   Observed wind profiles compared with the modified Peterson model.

All of the theories overestimated the speeds at the shorter fetches. One reason for this lies in the zero-plane displacement associated with the mustard. No theory takes into account the possible effects of such a displacement on the flow modification. At 10 m downwind from the discontinuity the flow had not yet descended fully onto the fallow; this is indicated by the fact that the upper four points of the profile fit best to a line that is based on a non-zero displacement length. At 20 m a line based on the roughness length alone fit the upper three points of the observed profiles. The flow descent seemed to be complete. However, at heights greater than 2 m there is little difference in the lines. Another possible reason for the discrepancy is the proximity to the discontinuity. Elliot's theory specifically applies at distances greater than 10^3 z_{02}, and most other models exclude the region where local pressure effects may be felt.

There did not appear to be an inflection point in the observed profiles. However, no firm conclusion could be reached on the basis of so few data points; a larger number would be necessary to detect a change in curvature. The lower portions of the profiles were more nearly logarithmic than the Peterson model predicted (Figs. 5,6). There is little difference in the profiles predicted by the other five theories. The simple Elliot solution provided a fit to the data as close as, or marginally better than, any of the more complicated solutions (Figs. 7,8).

d *Turbulence Statistics*
Existing data for the moments of the turbulent fluctuations are inexact, strongly scattered, incomplete, and do not agree well with each other. The explanation is evidently the considerable error in measurements of turbulent quantities that have quite large variability both in the vertical and the horizontal, even above a relatively homogeneous surface (Monin and Yaglom, 1971). The fast response data obtained at Chin made possible the calculation of the standard deviations of the vertical and longitudinal wind components. The vertical wind was measured by the sonic anemometer. The wind speed was measured by the vane-mounted horizontal propeller of the shear stress meter, and the standard deviation of the longitudinal component can be obtained from this if it is assumed that the statistics of the two variables are interchangeable (Lumley and Panofsky, 1964).

The characteristics of the vertical component near the ground are reasonably well understood; the theory is relatively simple because the proximity of the surface prevents low-frequency oscillations from forming. Furthermore, the normal roughness length serves to represent the terrain effect on the intensity of vertical turbulence (Lumley and Panofsky, 1964). There is no doubt that large-scale features are unimportant (Monin and Yaglom, 1971). In neutral conditions the standard deviation of the vertical velocity is proportional to the friction velocity

$$\sigma_w = A \, u_*$$

The value of the constant A, however, is a subject of much controversy. Estimates have ranged from 0.7 to 1.4. The mean value of all estimates from atmospheric observations lies in the range 1.2 to 1.3 while laboratory work suggests 0.9 (Monin and Yaglom, 1971). Lumley and Panofsky (1964) recommended the value 1.05. A short summary of estimates is included in Table 4. Monin-Obukhov similarity theory predicts

$$\sigma_w/u_* = F_1 \, (z/L)$$

where F_1 is a universal function of the stability parameter z/L. The nature of the variation with stability is likewise a subject of debate. Recent work suggests that the ratio is not dependent on stability except at large instabilities where a slow increase is noted (Bowne and Ball, 1970; Monin and Yaglom, 1971).

The standard deviation of the longitudinal component in neutral conditions is also proportional to the friction velocity
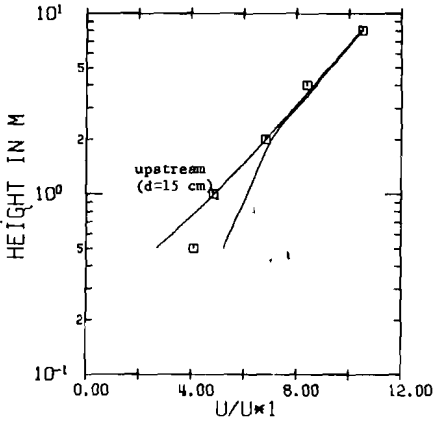
(a) Fetch 10 m, upstream profile with
zero-plane displacement
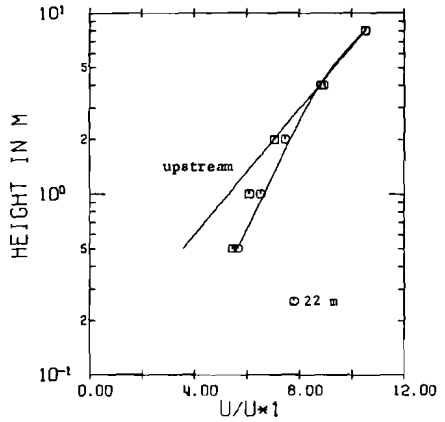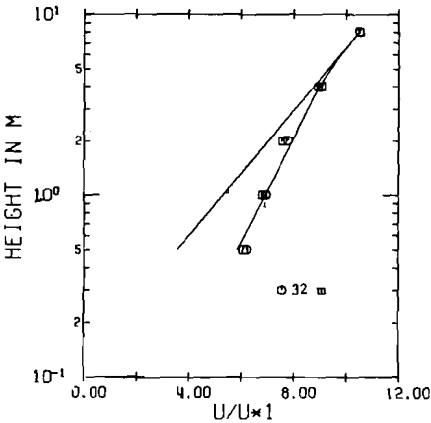
(b) Fetch 20 m

Fig. 7   Observed wind profiles compared with the theory of Elliot.

(a) Fetch 30 m
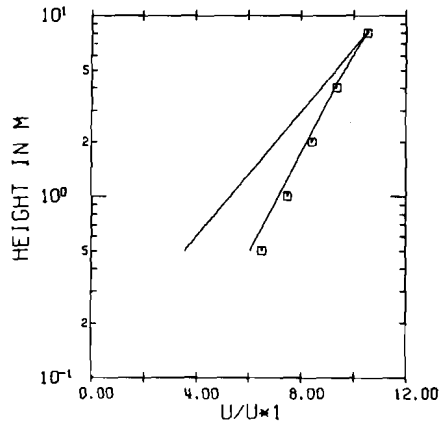
(b) Fetch 47 m

Fig. 8   Observed wind profiles compared with the theory of Elliot.

$$\sigma_u = B \, u_*$$

Estimates of the constant B have ranged from 2.1 to 3.0. Recent atmospheric data suggest a value 2.5 (Bowne and Ball, 1970) while laboratory work suggests the value 2.3 (Monin and Yaglom, 1971). A short summary of estimates is included in Table 5. There is evidence that the value varies with terrain (Lumley and Panofsky, 1964). Large-scale factors may well be important in addition to roughness. Again similarity theory predicts

$$\sigma_u/u_* = F_2 \, (z/L)$$

Variations with stability tend to be small, with perhaps a slight increase with increasing instability (Monin and Yaglom, 1971).

TABLE 4. Summary of values for ratio σ_w/u_*.

Value	Source
1.25	Panofsky and McCormick
1.33	Pasquill
0.7	Gurvich
0.87	Perepelkina
1.2	Klug
1.2	Panofsky and Prasad
1.2	Mordukhovich and Tsvang
1.3	Businger, Miyake, Dyer and Bradley
1.29	Busch and Panofsky
1.35	Haugen, Kaimal and Bradley
1.4	McBean
0.9–1.05	Laufer, Klebanoff, Comte-Bellot, Coantic
0.7–0.8	Cermak, Sandborn, Chuang
1.22	Kaimal and Izumi
1.1	Cramer
1.29	Bowne and Ball

TABLE 5. Summary of values for ratio σ_u/u_*.

Value	Site	Source
2.45	Various	Davenport
2.9	O'Neill	Lumley and Panofsky
2.5	Australia	Lumley and Panofsky
2.1	Brookhaven	Lumley and Panofsky
2.3	Tsimlyansk	Monin
2.2	Pipe flow	Lumley and Panofsky
3.0	O'Neill	Klug
2.3	Laboratory	Laufer, Klebanoff, Comte-Bellot, Coantic
2.0	Round Hill	Cramer
2.48	Fort Wayne	Bowne and Ball

Values of σ_w and σ_u were computed using a 15 minute averaging period to coincide with the nominal 15 minute recording interval of the mean wind speeds. Four such values were then averaged to produce an hourly figure. The corresponding hourly values for u_* were then used to calculate the ratios σ_w/u_* and σ_u/u_*. Twelve ratios on June 30, 1972 gave

$$\sigma_w/u_* = 0.94 \text{ with a standard deviation of } 0.05$$
$$\sigma_u/u_* = 2.9 \quad \text{with a standard deviation of } 0.4$$

The stability for the period of these measurements ranged from $z/L = -0.39$ to $z/L = -0.080$. Ten ratios on July 1, 1972 gave

$$\sigma_w/u_* = 0.96 \text{ with a standard deviation of } 0.18$$
$$\sigma_u/u_* = 2.2 \quad \text{with a standard deviation of } 0.2$$

Stability ranged from $z/L = -0.075$ to $z/L = -0.003$.

The ratio σ_w/u_* exhibited no significant difference for these two broad stability categories. The difference between the values for σ_u/u_* could be the effect of stability, but it is more likely the effect of large-scale properties of the

terrain since the wind blew from opposite directions on the two test days. The average value for the ratio σ_w/u_* is 0.95. This is closer to the early atmospheric estimate of Perepelkina (Lumley and Panofsky, 1964) and to the value for laboratory flows (Monin and Yaglom, 1971) than it is to other recent atmospheric determinations. The average value for the ratio σ_u/u_* is 2.6. This is near the value suggested by other recent atmospheric data.

4 Conclusion
The zero-plane displacement for mustard 55 cm high was found to be 15 cm, lower than might be expected from most empirical formulas. The roughness of the mustard was determined to be 12 cm, in close agreement with several estimates, notably the roughness element description formula of Lettau and the power law given by Sellers. The fallow was found to have a roughness of 1 cm.

The average value for the ratio σ_w/u_* was found to be 0.95, lower than other recent atmospheric estimates, but in close agreement with the value for laboratory flows. No variation with stability was apparent.

The average value for the ratio σ_u/u_* was found to be 2.6, similar to other recent atmospheric estimates. Some evidence of a dependence on large-scale terrain properties was present.

As the air flowed from the mustard to the fallow the surface friction velocity inferred from the wind at 0.5 m overshot initially and returned slowly to equilibrium. The wind profile in the lower part of the internal boundary layer was more nearly logarithmic than predicted by the Peterson model. No inflection point was detected below the interface. Similar results are reported by Petersen and Taylor (1973). The Elliot theory provided a reasonable description of the wind profile in the internal boundary layer.

Recommendations
According to the simple, elegant theory of Elliot the height of the internal boundary layer grows with the 4/5 power of distance from the discontinuity. The slope of the interface is about 1/10 for distances of micrometeorological interest. Realistically, of course, there must be a transition zone between the two profile regions. The more detailed measurements of Bradley (1968) revealed that the new logarithmic profile is established up to a height of about 1/20 the fetch. Thus, for wind profiles characteristic of surface roughness a height/fetch ratio of 1/20 is to be recommended. However, all indications are that the turbulence properties do not adjust as rapidly to the new surface. In boundary layer theory the constant-stress sublayer is usually taken to be about 10% of the complete boundary layer. By analogy a height/fetch ratio of 1/200 is recommended for representative measurements of turbulence.

University of Alberta. I would like to thank Dr. K.D. Hage, my supervisor, for his guidance; Dr. J. Honsaker for his aid in data processing; Mr. Bill Perry of Chin, Alberta for the use of his farm as an experimental site; Ed Lubitz, Kathy Lubitz and Fred McDougall for making the morning run; Dr. P.A. Taylor of the University of Southampton for providing his mixing-length program and preprints of his papers.

References

ANGLE, R.P., 1973: Airflow Modification Due to a Change in Surface Roughness. M.Sc. Thesis, University of Alberta, Edmonton.

BLOM, J., and L. WARTENA, 1969: The influence of changes of surface roughness on the development of the turbulent boundary layer in the lower layers of the atmosphere. *J. Atmos. Sci.*, 26, 255–265.

BOWNE, N.E., and J.T. BALL, 1970: Observational comparison of rural and urban boundary layer turbulence. *J. Appl. Meteor.*, 9, 862–873.

ELLIOT, W.P., 1958: The growth of the atmospheric internal boundary layer. *Trans. Amer. Geophys. Union*, 39, 1048–1054.

GEIGER, R., 1966: *The Climate Near the Ground*, Harvard University Press, revised fourth edition, 611 pp.

HONSAKER, J.L., F. MCDOUGALL, and D. ORACHESKI, 1972: Data acquisition system for eddy flux measurements. Paper presented to 6th annual congress of Canadian Meteor. Soc., University of Alberta, Edmonton.

LETTAU, H., 1969: Note on aerodynamic roughness parameter estimation on the basis of roughness element description. *J. Appl. Meteor.*, 8, 828–832.

LUMLEY, J.L. and H.A. PANOFSKY, 1964: *The Structure of Atmospheric Turbulence*, Interscience Publications, New York, 239 pp.

MONIN, A.S. and A.M. YAGLOM, 1971: *Statistical Fluid Mechanics*, MIT Press, Cambridge, Mass., 769 pp.

MUNN, R.E., 1966: *Descriptive Micrometeorology*, Academic Press, New York, 245 pp.

PANOFSKY, H.A. and A.A. TOWNSEND, 1964: Change of terrain roughness and the wind profile. *Quart. J. Roy. Meteor. Soc.*, 90, 147–155.

PAULSON, C.A., 1970: The mathematical representation of wind speed and temperature profiles in the unstable atmospheric surface layer. *J. Appl. Meteor.*, 9, 857–860.

PETERSEN, E.L. and P.A. TAYLOR, 1973: Some comparisons between observed wind profiles at Riso and theoretical predictions for flow over inhomogeneous terrain. *Quart. J. Roy. Meteor. Soc.*, 99, 329–336.

PETERSON, E.W., 1969: Modification of mean flow and turbulent energy by change in surface roughness under conditions of neutral stability. *Quart. J. Roy. Meteor. Soc.*, 90, 561–576.

PLATE, E.J. and A.A. QURAISHI, 1965: Modelling of velocity distribution inside and above tall crops. *J. Appl. Meteor.*, 4, 400–408.

PLATE, E.J., 1971: *Aerodynamic Characteristics of Atmospheric Boundary Layers*, AEC critical review series, US Atomic Energy Commission, 190 pp.

SELLERS, W.P., 1965: *Physical Climatology*, University of Chicago Press, 272 pp.

STEARNS, C.R., 1970: Determining surface roughness and displacement height. *Boundary Layer Meteor.*, 1, 102–111.

SUTTON, O.G., 1953: *Micrometeorology*, McGraw Hill Book Co. Inc., New York, 333 pp.

TAYLOR, P.A., 1969: On wind and shear stress profiles above a change in surface roughness. *Quart. J. Roy. Meteor. Soc.*, 95, 77–91.

TAYLOR, P.A., 1972: Some comparisons between mixing length and turbulent energy equation models of flow above a change in surface roughness. Paper presented

to Third Conference on Numerical Methods in Fluid Mechanics, Paris, July, 1972.

TAYLOR, R.J., 1962: Small-scale advection and the neutral wind profile. *J. Fluid Mech.*, 13, 529–539.

TOWNSEND, A.A., 1966: The flow in a turbulent boundary layer after a change in surface roughness. *J. Fluid. Mech.*, 26, 255–266.

CALL FOR PAPERS – TENTH ANNUAL CONGRESS

The Tenth Annual Congress and Annual General Meeting of the Canadian Meteorological Society will be held at Laval University, Quebec City, Quebec 26–27–28 May 1976. The theme of the congress will be *Observational Networks*. In addition to sessions on the theme, there will be the usual sessions on other topics in meteorology according to the papers submitted.

The new Oceanography Division of the CMS will be organizing sessions on physical, chemical and biological oceanography and on inland and coastal waters at this congress, as at the last, and we cordially invite contributions.

Titles and definitive abstracts (less than 300 words) should reach the Program Committee by *1 February 1976*. Papers on meteorology should be sent to Dr. Gaston Paulin, Service de la Météorologie du Québec, Ministère des Richesses Naturelles, 194 rue St-Sacrement, Québec, Québec. Papers on oceanography should be sent to Dr. C. Mann, Bedford Intitute of Oceanography, P.O. Box 1006, Dartmouth, Nova Scotia.

Information on registration, accommodation, etc. will be provided in due course. The chairman of the coordination committee is Dr. André P. Plamondon, Faculté de Foresterie, Université Laval, Québec, Québec.

NOTES AND CORRESPONDENCE

OPERATION LEECAT

P.F. Lester

Environmental Sciences Centre (Kananaskis)
The University of Calgary
Calgary, Alberta
T2N 1N4
and
J.I. Macpherson
Flight Research Laboratory
National Aeronautical Establishment
National Research Council of Canada
Ottawa, Ontario
K1A 0R6

During late March, 1975, a series of research flights known as Operation LEECAT was conducted over southwestern Canada and the northwestern United States. The purpose of this brief note is to summarize the LEECAT investigation for the benefit of interested scientists.

The impetus for operation LEECAT developed from the decision of the Royal Aircraft Establishment (RAE) at Farnborough, England to send a VC-10 to Western Canada to investigate the effects of mountain-induced Clear Air Turbulence (CAT) on aircraft. RAE plans were coordinated with the National Aeronautical Establishment (NAE) of the National Research Council of Canada (NRCC) and the NAE T-33 also participated in the program. Both the VC-10 and T-33 carried instrumentation capable of measuring and recording airspeed, height, horizontal wind velocity, pressure, temperature and the three components of true gust velocity. In addition, the VC-10 had nearly 100 strain-gauges at various locations throughout the aircraft.

The project study area encompassed western Alberta and British Columbia south of 53N and the northwestern United States, north of about 40N. For logistics reasons, the T-33 and the VC-10 were based at Calgary and Canadian Forces Base Comox, on Vancouver Island respectively. Flight procedures, communications and forecast schedules were coordinated with the Canadian and American air traffic control groups (ATS and ATC) and the Atmospheric Environment Service (AES).

The daily operational schedule included a morning meteorological forecast and flight area selection with take-off after 1800 GMT and six to eight hours of search, depending on the area selected. In order to optimize CAT search

procedures, options were left open for in-flight flight plan modifications on the basis of forecast updates and/or current pilot reports (PIREPS).

Actual CAT search procedures varied from day to day depending on the forecast and recommended flight area. Ideally, both aircraft would search in the same area in different altitude bands in a suspected layer until significant turbulence was contacted. If necessary, the VC-10 would be vectored into the turbulence region and the T-33 would fly parallel flight legs above and/or below in order to document the atmospheric structure and the extent of the turbulence. A major shift of the long wave pattern during the course of the experiment was accompanied by the movement of the belt of strong westerlies and associated CAT regions into the central U.S. On some occasions this situation would have caused the T-33 to exceed its limited range and CAT searches were carried out in separate areas.

With the cooperation of several agencies and universities, a number of parallel data-gathering activities were organized in conjunction with the air-craft flights and the chinook research project at the University of Calgary. These included a program of intensified PIREP collection with the cooperation of ATS, AES and the major commercial airlines; the acquisition of twice-a-day VHRR Visual and Infrared NOAA Satellite images from the National Environmental Satellite Service (NESS); a program of time lapse photography from the University of Lethbridge; and a series of transects with instrumented vans in south-western Alberta, immediately to the lee of the mountains, by personnel of the University of Calgary and the University of Alberta.

Although it is too early to discuss quantitative results, some qualitative high-lights can be given. To keep things in perspective, the LEECAT investigation can be examined from three different viewpoints:

1) *CAT effects on aircraft.* RAE scientists indicated that the time that the VC-10 spent in light turbulence was significant, however there were only a few instances of what could be called moderate and no cases of severe turbulence. The T-33 did contact a few patches of significant moderate turbulence (vertical accelerations up to 0.6 g).

2) *The nature of CAT and atmospheric structures.* There were at least three flight days on which quite interesting atmospheric structures were encountered. Two of the cases relate to the occurrence of CAT on the north side of a strong jet stream in the exit region. Both were 'ideal' patterns in terms of vertical and horizontal shears, one producing CAT through a deep layer. A curious feature of the second case was a persistent vertical wind shear of more than 20 knots per thousand feet. This shear was found in a nearby 1200Z Rawinsonde observation and was vertified a few hours later by aircraft measurements, however only a few patches of light to moderate turbulence were encountered.

The third case of note was an outbreak of light to moderate turbulence in a weak upper-level ridge. It is suspected that mesoscale horizontal shears were much larger and that the flow had a much higher degree of anticyclonic curvature than indicated by the rawinsonde network. This possibility will be examined in later analyses.

TABLE 1. Summary of operation LEECAT activities. March 17–25, 1975.

Date	Area	Levels (100's of feet)	Period (GMT)	Meteorological Conditions	Remarks
March					
17	Southern British Columbia Southern Alberta	180–340	1800–0000	Well defined chinook arch cloud, moderate vertical and horizontal wind shears, weak lee wave activity.	Light turbulence in vicinity of arch cloud.
18	Northern Montana	280–420	1800–0000	North side of 140 kt jet in exit legion weak lee wave activity.	Occasional light turbulence at several levels between 330 and 390, especially northeastern Montana.
19	Eastern Washington Northern Oregon Central Wyoming	190–410	2100–0200	North side of strong jet, weak lee wave activity.	A few patches of light to moderate turbulence between 190 and 290
20	Southern Idaho Southern Montana Wyoming Northern Colorado	140–340	1830–0300	Strongly sheared layer at lower levels, moderate vertical shears at higher levels, weak lee wave activity.	No significant turbulence.
21	Southern British Columbia	220–310	1830–0000	Weak upper ridge.	Wide area of light and moderate turbulence and temperature fluctuations at several levels. Aircraft flew a side-by-side calibration flight during this period.
23	Oregon	190–380	1900–0000	Very strong vertical shears (67 kts/3,000 feet) near jet axis.	A few patches of light to moderate turbulence (VC-10 only).
24	Southern British Columbia	160–350	2130–0000	Weak lee wave activity.	No significant turbulence. Evidence of lee waves in temperature structure at 160 (T-33 only).
25	Southern British Columbia	230–290	1930–2130	Weak lee wave activity.	No significant turbulence (T-33 only).

3) *Chinook research.* Although there was no extensive chinook activity during the period of the aircraft flights, two marginal situations did occur. In addition to the aircraft flights, observations included surface transects and time-lapse photography. Flight data were gathered in the vicinity of a chinook arch cloud which was also visible in NOAA Satellite imagery. It should also be mentioned that a few PIREPS from commercial aircraft in the Medicine Hat–Cranbrook area provided evidence of very long lee wave activity.

An overall summary of LEECAT is presented in Table 1. General flight areas and approximate flight times are included. Data analyses are being conducted at RAE, NAE and the University of Calgary. Any questions regarding the availability and format of the data may be addressed to either of the authors.

In conclusion, a very satisfying aspect of LEECAT was the cooperation of several groups from several different geographical areas. Despite the short lead time, this cooperation allowed the organization of an intense scientific effort. All directly associated with LEECAT wish to express their thanks to the many people and organizations who gave their support during the course of the experiment.

CONTRIBUTIONS SCIENTIFIQUES AU DIXIEME CONGRES ANNUEL

La fin de mai 1976 sera marquée par la tenue du dixième congrès annuel et de la réunion générale annuelle de la Société météorologique du Canada dans la ville de Québec. Les dates exactes du congrès sont 26–27–28 mai 1976. *Les réseaux d'observation* sera le thème central du prochain congrès. Toutefois, suivant la coutume, plusieurs autres sujets en météorologie pourront être présentés après soumission.

Pour la deuxième année consécutive, la division nouvelle d'Océanographie à la S.M.C. organisera des sessions traitant de l'océanographie physique, chimique et biologique et des eaux intérieures ou côtières. Nous espérons recevoir de nombreuses contributions scientifiques dans ce domaine.

Les titres ainsi que les sommaires définitifs (300 mots ou moins) devront parvenir au comité du programme d'ici le *1er février 1976.* Les textes scientifiques en météorologie devront être envoyé au Dr Gaston Paulin, Service de la Météorologie du Québec, Ministère des Richesses naturelles, 194, Ave St-Sacrement, Québec, tandis que ceux en océanographie devront être envoyés au Dr. C. Mann, Bedford Institute of Oceanography, P.O. Box 1006, Dartmouth, Nova Scotia.

Les informations sur l'inscription, l'hébergement, etc seront disponibles prochainement. Le président du comité de coordination est Dr André P. Plamondon, Faculté de Foresterie, Université Laval, Québec, Québec.

BOOK REVIEWS

REVIEW OF URBAN CLIMATOLOGY 1968–1973. T.R. Oke. Technical Note No. 134, WMO, Geneva, WMO – No. 383, 1974, 132 pp.

Since the WHO/WMO Symposium on Urban and Building Climatology (Brussels, 1968), the literature in the field of urban climatology has expanded rapidly. Dr. Oke's critical review of the development in this field subsequent to the 1968 symposium is therefore both timely and welcomed. Significant new advances and problem areas, as well as topics for future research pertaining to the understanding of the processes underlying the nature of urban climate are summarized. It should be noted that the scope of this review does not include substantially the field of urban air pollution.

The report consists of five sections, namely, radiation balance, water balance, energy balance, climatological effects, and energy and circulation models. The material, as the author states, is "sequentially organized in the order in which one normally hopes to approach analysis of a boundary-layer environment". Observational studies are dealt with in the first four sections, starting first with the cascades of energy and mass through the city-atmosphere system. The resultant climatological effects (temperature, humidity and wind speed) are then treated. In the last section, a fairly comprehensive review is made of attempts to model the workings of urban climate.

This report, which includes an extensive bibliography (377 references), is well-organized and written. A few diagrams or illustrations to supplement the text would, however, have been useful. It should prove to be a valuable reference document for researchers in urban climate.

D. Yap
Air Resources Branch
Ontario Ministry of the Environment
Toronto, Ontario

ATMOSPHERIC DIFFUSION (2nd Edition) F. Pasquill. Halsted Press (a division of John Wiley & Sons) New York, London, Sydney and Toronto, 1974, 429 pp, $39.75. (U.S.)

This book by Pasquill is subtitled "The Dispersion of Windborne Material from Industrial and other Sources". As the subtitle implies, the book is ultimately concerned with the means of estimating the vertical and horizontal spread of a plume in a turbulent atmosphere. The current edition represents an extensive revision of the 1961 edition which is a standard reference in the libraries of most diffusion meteorologists. There are over a hundred more pages in this edition which contains references to about 180 papers that have been published since 1961. The main emphasis of the book may perhaps be evaluated by comparing the small number of referenced papers which have been published in operationally biased journals such as the Journal of the Air Pollution Control Association (seven references, none more recent than 1968) and the Journal of Applied Meteorology (10 references, only one more recent than 1967) with the large number of referenced papers which were published in the more philosophically biased Quarterly Journal of the Royal Meteorological Society (75 references).

The book has six chapters, the first of which contains an introduction and a brief outline.

A discussion of the properties of atmospheric turbulence is contained in Chapter 2. The statistical properties of turbulent flow are introduced and the effects of finite sampling and averaging are discussed. Basic concepts are elaborated upon: eddy diffusivities, similarity arguments, Richardson number, gradient transfer relations, isotropic turbulence, and the overall shape and scale of turbulent wind fluctuation spectrums. Theory is developed to show how the vertical component of the wind fluctuations can be systematically related to such factors as wind speed, the nature of the terrain and the stability of the atmosphere. This development lends insight into the expected behaviour of vertical plume diffusion. Finally there is a detailed theoretical examination of the relation between Lagrangian and Eulerian fluctuations. This examination leads to the introduction of the Lagrangian/Eulerian scale ratio β which is of basic importance to practical diffusion work.

Much of the third chapter is devoted to a discussion of the strength and shortcomings of the three basic theoretical approaches which are used to predict plume diffusion: gradient-transfer theory, similarity theory and statistical theory. Gradient-transfer theory appears to be acceptable

for explaining the vertical diffusion of a plume originating from a ground-based source under neutral atmospheric conditions. It is pointed out that care should be exercised in applying it to other problems. Without valid physical justification this approach can degenerate to nothing more than arbitrary formula fitting. Similarity theory is a promising basis for predicting plume diffusion at short distances from a ground-level source. Statistical theory allows one to estimate the vertical and horizontal spread of an elevated plume from wind fluctuation data. (It is incidentally with the statistical theory of turbulence that Pasquill has perhaps made his major contributions to the understanding of diffusion processes). This third chapter also contains theoretical discussions relating to the expanding cluster, the diffusion of falling particles and the effect of wind shear on horizontal plume spread.

Chapter 4 contains the results of experimental studies of basic features of atmospheric diffusion. Observational techniques for evaluating atmospheric diffusion properties are discussed. Results of various experiments are commented upon. It is concluded that the average cross wind distribution of concentrations in a plume may be assumed to be Gaussian. Evidence is presented to show that the statistical theory of turbulence may be adequately employed to predict crosswind spread of a plume. It is also shown that the vertical spread of an elevated plume may be usefully represented by a statistical treatment of wind fluctuation data. The vertical distribution within an elevated plume is effectively Gaussian. Vertical plume spreads from a ground-based source may be estimated from gradient transfer theory or similarity theory. The shape of the vertical distribution of such plumes is probably not Gaussian. Discussions are also given concerning the growth of clusters of particles and concerning large scale diffusion.

The distribution of windborne material from real sources is considered in Chapter 5. A wide variety of topics is included: formulas for predicting plume rises in different atmospheric conditions (Pasquill seems to be partial to the $^2/_3$ law formula for neutral conditions), deposition of airborne material, washout in rain, long-term distributions around an isolated source, fumigation, effects of buildings, urban air pollution and the budget of sulphur dioxide over a large area.

The sixth and final chapter discusses the means of estimating diffusion and air pollution from meteorological data. The Gaussian plume model is generally recommended for use in evaluating point source emissions. Pasquill emphasizes that the adoption of this model for practical purposes is not crucial but rather a matter of convention and convenience. This chapter contains an updated version of Pasquill's celebrated method for evaluating plume diffusion according to categories which are determined by the readily available meteorological parameters of insolation, cloud cover and wind speed. It also contains brief discussions of urban modelling approaches such as the well known Gifford-Hanna approach, the box model approach and the grid-cell systems approach. The chapter and book ends with a consideration of the generally poor accuracy achieved with the present means of estimating air pollution from meteorological data. Uncertainties in individual situations are often factors of two or more. Pasquill concludes "It remains to be seen whether any significant improvement in the situation will evolve as a consequence either of the ever-increasing sophistication in the studies of atmospheric flow or of the growing tendencies for elaboration in modelling techniques. For the moment there are no obvious signs of such improvement."

The book assumes that the reader is already at an advanced level of sophistication with respect to mathematical knowledge and meteorological experience. It will be valuable for any one concerned with acquiring a basic knowledge of diffusion theory. It may be a disappointment for meteorological engineers. Much of the discussions pertaining to matters of practical interest are limited. For example, in the treatment of the half-life of sulphur dioxide in the atmosphere the most recent article referred to was published in 1963. The discussions of urban air pollution do not refer to the urban heat island, a phenomenon which is usually associated with the poorest urban air quality. The question of avoiding building downdraught effects is considered by reference to the discredited $2^1/_2$ times rule. There are no substantial discussions of such important current topics as irregular terrain effects, plume trapping (not to be confused with fumigation), cooling-tower plumes and atmospheric chemistry.

The price of the book, $39.75, reflects the current levels of inflation. It will, however, make a worthwile investment for those scientists who do not possess the first edition.

<div align="right">
D.M. Leahey
Western Research and Development Ltd.
Calgary, Alberta
</div>

NUCLEAR METEOROLOGY. Edited by K.P. Makhon'ko and S.G. Malakhov, translated from the Russian by the Israel Program for Scientific Translations, Jerusalem 1974. International Scholarly Book Services Inc, Box 4347, Portland, Oregon 97208, $32.00 (U.S.)

It would be almost impossible to think of a less appropriate title for this book. The meteorologist might be excused for thinking it dealt with nucleation, or at least had some slight connection with meteorology. Not so. The nuclear physicist will likewise be baffled for it contains no nuclear physics. Reactor safety experts might be led to expect a treatment of meteorological aspects of the siting of nuclear reactors, but they will be disappointed. The publishers are not really to blame for the book is a translation of the proceedings of the All Union Conference on Nuclear Meteorology held at Obinsk in 1969, but the conference was really all about environmental radioactivity and this would certainly have been a more apt title for both the conference and its proceedings.

The chapter titles are as follows:
1. Global pollution of the atmosphere and fallout of nuclear blast products
2. Accumulation of radioactive products of nuclear blasts on the underlying surface
3. Radioactive particles during nuclear bursts in the troposphere
4. Processes of atmospheric scavenging
5. Natural radioactivity of the atmosphere
6. Equipment and methods for the study of radioactive contamination in the environment.

The book thus covers quite a wide range of topics and it would be surprising if nearly everyone working, however remotely, in the general field did not find something of interest in it, but that is about as far as one can go in recommending it. Also, it is all a bit old. One continually finds statements such as 'New data (for the period 1967–1968) are examined . . . .' and one has the feeling that most of the work reported has been overtaken by other work which has, moreover, been published long ago. This is a perennial difficulty in the publication of conference proceedings, especially when translation is necessary and one is loath to criticise the monumental efforts of the Israel Program for Scientific Translations on that account. The translation itself appears excellent and there is a remarkable lack of errors and misprints.

<div style="text-align: right">

W.J. Megaw
York, University
Toronto, Ontario

</div>

CALL FOR NOMINATIONS – 1975 AWARDS

Nominations are requested from members and Centres for the 1975 CMS Awards to be presented at the 1976 Annual Meeting. Four awards are open for competition: 1) the President's Prize for an outstanding contribution in the field of meteorology by a member of the Society; 2) the Prize in Applied Meteorology, for an outstanding contribution by a member in that field; 3) the Graduate Student Prize, for a contribution of special merit, and 4) the Rube Hornstein Prize in Operational Meteorology, for outstanding service in providing operational meteorological service. The awards will be made on the basis of contributions during the 1975 calendar year, except 4) which may be awarded also for work performed over a period of years.

Nominations are also requested for the award of citations to individuals or groups in Canada who have made some outstanding contribution in helping to alleviate pollution problems or in developing environmental ethics.

All nominations should reach the corresponding secretary not later than *March 1, 1976.*

APPEL AUX CANDIDATURES POUR LES PRIX ET CITATIONS 1975

On demande aux membres et aux centres locaux de soumettre leurs nominations aux candidatures pour les prix de la Société pour l'année 1975. Il y a quatre prix: 1) le prix du président pour un travail exceptionnel en météorologie par un membre de la Société, 2) le prix de météorologie appliquée pour un travail exceptionnel dans ce domaine par un membre, 3) le prix aux étudiants gradués et 4) le prix de météorologie opérationnelle Rube Hornstein pour un travail exceptionnel dans l'exploitation des services météorologiques.

Tous les prix seront attribués pour un travail qui a été effectué durant l'année 1975, à l'exception de 4) qui peut aussi être attribué pour un travail effectué durant une période couvrant plusieurs années.

On demande aussi des nominations des candidats susceptibles de se voir décerner une citation par la Société. Une citation peut être décernée à un individu ou à un groupe qui a apporté une contribution exceptionnelle à la solution des problèmes de la pollution, à l'amélioration de l'environnement ou au développement d'une éthique écologique.

Toutes les nominations recueillies par le secrétaire-correspondant avant *le 1er mars 1976* seront remises aux comités des récompenses et des citations, selon le cas.

The Canadian Meteorological Society / La Société Météorologique du Canada

The Canadian Meteorological Society came into being on January 1, 1967, replacing the Canadian Branch of the Royal Meteorological Society, which had been established in 1940. The Society exists for the advancement of Meteorology, and membership is open to persons and organizations having an interest in Meteorology. At nine local centres of the Society, meetings are held on subjects of meteorological interest. *Atmosphere* as the scientific journal of the CMS is distributed free to all members. Each spring an annual congress is convened to serve as the National Meteorological Congress.

Correspondence regarding Society affairs should be directed to the Corresponding Secretary, Canadian Meteorological Society, c/o Dept. of Meteorology, McGill University, P.O. Box 6070, Montreal, P.Q. H3C 3G1

There are three types of membership – Member, Student Member and Sustaining Member. For 1975 the dues are $20.00, $5.00 and $60.00 (min.), respectively. The annual Institutional subscription rate for *Atmosphere* is $15.00.

Correspondence relating to CMS membership or to institutional subscriptions should be directed to the University of Toronto Press, Journals Department, 5201 Dufferin St., Downsview, Ontario, Canada, M3H 5T8. Cheques should be made payable to the University of Toronto Press.

La Société météorologique du Canada a été fondée le 1er janvier 1967, en replacement de la Division canadienne de la Société royale de météorologie, établie en 1940. Cette société existe pour le progrès de la météorologie et toute personne ou organisation qui s'intéresse à la météorologie peut en faire partie. Aux neuf centres locaux de la Société, on peut y faire des conférences sur divers sujets d'intérêt météorologique. *Atmosphere*, la revue scientifique de la SMC, est distribuée gratuitement à tous les membres. À chaque printemps, la Société organise un congrès qui sert de Congrès national de météorologie.

Toute correspondance concernant les activités de la Société devrait être adressée au Secrétaire-correspondant, Société météorologique du Canada, Département de Météorologie, l'Université McGill, C.P. 6070, Montréal, P.Q. H3C 3G1

Il y a trois types de membres: Membre, Membre-étudiant, et Membre de soutien. La cotisation est, pour 1975, de $20.00, $5.00 et $60.00 (min.) respectivement. Les Institutions peuvent souscrire à *Atmosphère* au coût de $15.00 par année.

La correspondance concernant les souscriptions au SMC ou les souscriptions des institutions doit être envoyée aux Presses de l'Université de Toronto, Département des périodiques, 5201 Dufferin St., Downsview, Ontario, Canada, M3H 5T8. Les chèques doivent être payables aux Presses de l'Université de Toronto.

Council / Conseil d'Administration: 1975–76